

Genetic and functional diversity of allorecognition receptors in the urochordate, *Botryllus schlosseri*

Henry Rodriguez-Valbuena^{1,a}, Jorge Salcedo¹, Olivier De Their², Jean Francois Flot², Stefano Tiozzo^{2,b}, Anthony W De Tomaso^{1,c}

¹Molecular, Cellular and Developmental Biology, University of California, Santa Barbara, CA, USA.

²Evolutionary Biology & Ecology, C.P. 160/12, Université libre de Bruxelles (ULB), Avenue F.D. Roosevelt 50, B-1050 Brussels, Belgium

³CNRS, Laboratoire de Biologie du Développement de Villefranche Sur-mer (LBDV), Sorbonne Université, Paris, France.

a <https://orcid.org/0000-0002-2687-0333>

b <https://orcid.org/0000-0003-2822-2783>

c <https://orcid.org/0000-0001-9689-7673>

Corresponding author: Anthony De Tomaso: awdeto@ucsb.edu

Abstract

Allorecognition in *Botryllus schlosseri* is controlled by a highly polymorphic locus (the *fuhc*), and functionally similar to missing-self recognition utilized by Natural Killer cells- compatibility is determined by sharing a self-allele, and integration of activating and inhibitory signals determines outcome. We had found these signals were generated by two *fuhc*-encoded receptors, called *fester* and *uncle fester*. Here we show that *fester* genes are members of an extended family consisting of >37 loci, and co-expressed with an even more diverse gene family- the *fester co-receptors (FcoR)*. The *FcoRs* are membrane proteins related to *fester*, but include conserved tyrosine motifs, including ITIMs and hemITAMs. Both genes are encoded in highly polymorphic haplotypes on multiple chromosomes, revealing an unparalleled level of diversity of innate receptors. Our results also suggest that ITAM/ITIM signal integration is a deeply conserved mechanism that has allowed convergent evolution of innate and adaptive cell-based recognition systems.

Keywords: allorecognition, innate immune receptors, haplotype variation, alternative splicing, tunicates, NK-cells

Introduction

Highly polymorphic allorecognition systems are found in species throughout the metazoa, and studies on allogeneic transplantation led to the discovery of both adaptive and innate cell-based recognition systems in vertebrates^{1,2}. Discriminatory ability in adaptive immunity is based on somatic recombination and thymic selection, identifying TCRs with structures that can discriminate between even a single residue on a pMHC complex^{3,4}. Innate allorecognition is mediated by NK cells, which tally binding from a repertoire of stochastically expressed activating and inhibitory receptors to determine the health of a target cell⁵. Inhibitory receptors bind to polymorphic epitopes on MHC Class I allotypes, allowing NK cells to determine their presence or absence, a strategy called missing-self recognition²

Both innate and adaptive receptors utilize the same signaling pathways- the TCR and NK activating receptors use the ITAM pathway, while inhibitory receptors in both cells use the ITIM pathway, and discrimination is due to an interaction between kinase and phosphatase activity⁶⁻⁸. Finally, during development both cells go through a cell autonomous education process, which quantifies binding potential and sets an activation threshold that allows cells to be self-tolerant and functional^{4,9,10}.

Interestingly, T-cell recognition appears as a functioning unit in jawed vertebrates- but no homologs of the MHC, TCR, RAG, or evidence of thymic selection have ever been identified in jawless fish, non-vertebrate chordates, or invertebrates^{11,12}. NK receptors are evolving even faster: rodents use the C-type lectin *Ly49* genes, while the primate analogs are the Killer cell immunoglobulin-like receptors (*KIRs*)¹³- and neither are found outside of the mammals¹⁴. This plasticity is not restricted to vertebrates- histocompatibility has been characterized in three non-vertebrate clades, and in each, candidate genes also emerge abruptly, with no homologs found outside of closely related species¹⁵⁻¹⁷. However, both vertebrate and candidate non-vertebrate allorecognition receptors are part of multigene families encoded in polymorphic haplotypes^{14,15,18,19}, and activating and inhibitory members encoding ITAM and ITIM signaling motifs are found in both the cnidarian, *Hydractinia*¹⁹ and *Botryllus* (this study). The recurring evolution of both vertebrate and non-vertebrate recognition systems that all converge onto equivalent signaling pathways suggest that the cellular mechanisms that process information from cell surface binding events are conserved, allowing receptors to evolve freely²⁰.

Botryllus schlosseri is a urochordate, the sister group to the vertebrates²¹, and provides a novel model to investigate mechanisms underlying polymorphic discrimination and the evolution of vertebrate immunity. *Botryllus* undergoes a natural transplantation reaction when two individuals grow into proximity. Terminal projections of the vasculature, called ampullae come into contact. If two individuals are compatible, the ampullae will *fuse*, forming a parabiosis. If they are incompatible, the vessels will *reject*, an inflammatory reaction which prevents vascular fusion (Extended Data Fig. 1). Fusion or

rejection is controlled by a single, highly polymorphic locus called the *fuhc* (**f**usion/**h**istocompatibility) and discrimination occurs by missing-self recognition- individuals are compatible if they share one or both *fuhc* alleles, but are incompatible if no alleles are shared^{11,22}.

Botryllus populations have 200-500 *fuhc* alleles, thus the effector system can pinpoint a self-allele from hundreds of competing nonself alleles^{23,24}, but the mechanisms that allow an innate recognition system to carry out this level of discrimination are not understood. We had previously characterized two histocompatibility receptors encoded in the *fuhc* locus: *fester* is highly polymorphic and required for fusion, while *uncle fester* is monomorphic and is required for rejection^{25,26}. Similar to NK cell recognition, the outcome is due to an interaction between these two independent pathways, however, neither gene encodes known signaling domains, and it was unclear if other receptors contributed to specificity.

Here we find that rather than being encoded in only two loci, the *fester* genes are part of a large, multigene family, and co-expressed with members of another multigene family- the *fester coreceptors* (*FcoR*). *FcoR* are type I transmembrane proteins that encode ITIM and hemITAM motifs. These results suggest that two families of immune receptors participate in the *Botryllus* histocompatibility response, and that polymorphic discrimination requires an interaction between ITAM and ITIM signaling.

Results

***fester* and *uncle fester* are members of a large gene family**

fester and *uncle fester* share a similar domain structure (Fig. 1a,c), but amino acid similarity is only found in the COOH half of the protein, encoding the TM and intracellular domains. We identified low homology structural homologs of *fester* in the *fuhc* locus of a related ascidian²⁷, and used those to search in 26 transcriptome and four genome databases of *Botryllus* (Extended Data Table 1), and identified 45 unique sequences (Fig. 1a, b Extended Data Fig. 2a). On average, these sequences shared 20% identity at the amino acid level (Extended Data Fig. 2a, b), which was concentrated in the COOH tail half of the protein.

To estimate which of these sequences were alleles vs loci, we used the range of protein identity values from a population genetic study of *fester* as a benchmark (Extended Data Fig. 2b)²⁸. If sequences shared >82% amino acid homology and >90% nucleotide homology over the entire gene, they were classified as alleles, predicting 37 new loci. We are calling these new genes the *fester* family (FF), and *fester* and *uncle fester* have been renamed FF1 and FF3, respectively. Phylogenetic analysis (Fig. 1b) sorted these loci into multiple clades. Each individual expressed a nearly unique repertoire of *fester* genes, with an average of 10 *fester* genes or alleles per individual, with a range of 7-13 (Extended Data Fig. 3, Table 3), suggesting that FF loci are encoded in complex haplotypes with presence/absence polymorphisms.

Genetic properties of the fester family members

The genes encoding the FF1 and FF3 are composed of eleven and nine exons, respectively (Extended Data Fig. 4a). Each gene shares a common overall structure: exon one encodes a signal sequence, a Sushi domain is encoded on exon 5 (FF1) and 3 (FF3), and in both cases the Sushi domain is followed by two short exons that encode extracellular regions, followed by three exons, each encoding one transmembrane domain^{25,26}. We determined the genomic structure for nine other *fester* family members, and they are encoded in 9, 10, or 12 exons, with a similar exon architecture in the center of the gene as described above. (Extended Data Fig. 4a).

We had previously found that FF1 is highly polymorphic, identifying 60 allotypes in the U.S.²⁸. In contrast, FF3 was nearly monomorphic, as only two alleles that differed by a single amino acid were identified²⁶. Of the 37 new loci, three are polymorphic (FF12, FF13 and FF28), but not to the level of FF1. These three loci each have 3-4 alleles that are ca. 90% identical. In contrast, 14 of the new loci were clearly monomorphic, as identical nucleotide sequences were identified in > 5 individuals.

However, as almost half of the unique sequences were present in only one or two individuals (Extended Data Table 3), this is likely an underestimate. Nevertheless, many of the new loci are monomorphic.

Alternative splicing in the extracellular and intracellular regions of fester genes

One common characteristic of the known fester genes was the alternative splicing of two extracellular exons following the Sushi domain, moving that exon relative to the plasma membrane (Fig. 1a). We found that 26 of the new loci showed equivalent patterns in the extracellular region (Extended Data Fig. 4a and Table 5). Alternative splicing was also detected in the cytoplasmic tail of 12 fester genes (Extended Data Fig. 4a and Table 5). These splice variants generate new stop codons, changing the structure of the cytoplasmic tail, which may affect interactions with other proteins (described below).

FF genes diversify by intergenic recombination

Fester family members have high similarity in their C-terminal regions, but low similarity in their extracellular regions (Fig 1a). To characterize the evolution of these regions, we analyzed the extracellular and intracellular (transmembrane and cytoplasmic) regions of the fester proteins independently (Fig. 2a,b). Analysis of the intracellular region identified five well supported clades (Fig. 2b). However, most of the ectodomains of the same fester loci split into different clades when analyzed independently (Fig. 2a), suggesting that the fester genes are diversifying by intergenic recombination, mixing and matching the ectodomains and intracellular domains. However, one clade of fester genes did not exhibit intergenic recombination (orange in Fig. 2a,b). As discussed below, this is a result of the presence of two separate clusters of FF genes, restricting the recombination of extracellular and intracellular regions to the genes encoded on the same chromosome (Fig. 4).

Identification of the fester co-receptor (FcoR) gene family

Our search for new fester genes also identified another group of conserved sequences located in the *fuhc* locus. These genes encoded a type I protein with a single transmembrane domain (Fig. 1c; Extended Data Fig. 4b), and ranged in size from 520-610 aa. They also encoded canonical ITIMs, hemITAMs and other signaling motifs in their cytoplasmic tails. We are tentatively naming these genes the Fester co-receptors (FcoRs).

The FcoR genes are even more diverse than the FF genes, and we identified 69 unique sequences in the same databases (Extended Data Fig 2c). Nine were full length, encoding a signal peptide and stop codon, 37 were nearly fully length and had a predicted TM, intracellular tail and most had a stop codon (Extended Data Fig. 6). We also found 23 partial sequences that overlapped with the extracellular region of the full-length sequences. As described below, one of these loci (FcoR7) was highly

polymorphic, and we used the same analysis as for fester to estimate that there are 53 unique FcoR loci (Extended Data Fig. 2c,d). Each individual expressed an almost unique repertoire of FcoR genes (Extended Data Fig. 8; Table 3), with an average of 14 FcoR genes/individual, and a range of 4 to 28 genes expressed/individual (Extended Data Fig 3).

Similar to the FF loci, the FcoR genes diversify both genetically and somatically, however phylogenetic analysis revealed that the FcoR genes were more complex than the FF genes (Fig. 1d). The FcoR genes grouped into multiple clades, and independent analysis of the ectodomain and TM/intracellular region also showed that these genes diversify via intergenic recombination (Fig. 2c,d). However, the TM/intracellular region of the FcoR genes were more diverse than the FF genes with a higher number of clades in the phylogenetic analysis.

We also found alternative splicing in the extracellular and intracellular regions of FcoR genes (Extended Data Fig. 4b). The most common splicing variant consisted of a deletion upstream of the transmembrane domain, creating a shorter variant of the ectodomain. We also found less common splicing variants, including one that deletes a fragment of the exon that encodes the transmembrane domain, as well as several in the cytoplasmic tail (discussed below).

Polymorphism of FcoR genes

Polymorphism of the FcoR genes mirrored results from the fester genes. One locus (FcoR7) was highly polymorphic, and we identified 20 allotypes that were 94% identical, with the polymorphisms concentrated in the extracellular region (Extended Data Fig. 2c,d; 5b). Three other polymorphic loci (FcoR2, FcoR3 and FcoR4) were also identified, and were similar to the oligomorphic FF loci (FF12, FF13 and FF28), in that they had 2-3 more divergent alleles (ca. 90% identity, Extended Data Fig. 2c, Table 3). There were also many monomorphic FcoR loci ($n > 5$; Extended Data Table 3). In summary, the patterns seen in the FcoR family are equivalent to the FF family, with the same caveat that almost half of the unique FcoR sequences were present in only one or two individuals.

FcoRs encode canonical ITIMs, hemITAMs and other tyrosine motifs in the intracellular tails

Every FcoR protein sequence with a transmembrane domain and cytoplasmic tail longer than 100 aa encoded one or more tyrosine-based motifs (Extended Data Fig. 6). Some genes encoded a canonical Immunoreceptor Tyrosine-based Inhibitory Motif (ITIM: I/L/VxYxxI/L/V), others encoded a canonical hemi-Immunoreceptor Tyrosine-based Activation Motif (hemITAM: [E/D][E/D][E/D]xYxxL), and one had an Immunoreceptor Tyrosine-Switch Motif (ITSM: TxYxxI)²⁹. Almost all the sequences encoded a tyrosine core motif (YxxI/L/V)²⁹. About half of the core motifs had an acidic amino acid at -2 position, and a valine at -1 position ([E/D]VYxxI/L/V), while the other half had no conservation prior to the

tyrosine. Several of the sequences also encoded predicted SH2 (Src Homology 2) motifs. Many of the loci encoded multiple motifs, although there was no clear pattern of pairings nor spacing between them (Extended Data Fig. 6).

Two of the polymorphic loci (FcoR3 and FcoR4) encoded alleles that differed in the cytoplasmic tail and swapped the ITIM and hemITAM domains in nearly the same pattern (Fig. 3.). For FcoR4, one of the alleles (FcoR4B) encoded a canonical ITIM motif (LAYAIV) and a partial hemITAM motif (PDDVYAIL), while the other allele (FcoR4A) had a substitution on the ITIM motif (FAYAIV), and encoded a canonical hemITAM (EDDVYAIL) (Fig. 3). We also found an alternative splice of FcoR4A in multiple individuals which retained intron 12. This new sequence encoded an ITIM domain (VIYMTI) and excluded the hemITAM (Fig. 3a). Thus, there are activating and inhibitory alleles of the same locus, and these can also be switched by alternative splicing.

FcoR3 had an equivalent allelic pattern but was even more diverse, as multiple alternative splice variants were found that modified the signaling motif repertoire (Fig. 3b). Together the data suggests that FcoR can be classified into activating, inhibitory and neutral receptors, and moreover genes can switch motifs via both allelic polymorphism and alternative splicing. Finally, every individual expressed one or more FcoR genes with an ITIM motif, one or more with a hemITAM motif, and one or more with a tyrosine core motif (Extended Data Table 3).

Co-expression and physical mapping of the FF and FcoR loci

Interestingly, in over half the cases the expression of each FF locus was accompanied by a cognate FcoR locus (Extended Data Fig. 7 and Table 3). We found 14 pairs where loci of the two gene families were co-expressed over 80% of the time in 3 or more individuals, and for five of those the correlation was absolute (Extended Data Fig. 7, Table 3). However, it was the pairings themselves that were striking. Three of the polymorphic FF loci were expressed as pairs with three of the polymorphic FcoR loci, including the two most polymorphic family members (FF1 and FcoR7); as well as two of the less polymorphic family members (FF12 and FcoR3; FF13 and FcoR4). All the alleles of FcoR7 encode an ITIM motif, while both FcoR3 and FcoR4 have alleles with an ITIM motif (Fig.3, Extended Data Fig. 6). The pairing of the only highly polymorphic loci of each family- FF1 and FcoR7, is consistent with our previous functional studies, which suggested the FF1 was part of an inhibitory receptor that discriminated between fuhc ligands, as it was required for fusion²⁵. In addition, the pairing of the other polymorphic FF with FcoR loci encoding an ITIM is consistent with the idea that the polymorphic FF loci would be involved in specificity, and thus be inhibitory receptors in a missing-self recognition event.

In contrast, functional data suggested that the monomorphic FF3 was an activating receptor²⁶, and it pairs with monomorphic FcoR1, which encodes a core tyrosine motif in the intracellular tail (Extended

Data Fig. 6c, 7b). In the remaining ten pairs both loci are monomorphic and the FcoR partner encodes a core tyrosine motif.

Physical mapping of the FF and FcoR loci revealed that co-expression patterns correlated with genomic linkage of the two genes (Fig. 4 and Extended Data Fig. 7). We initially mapped the new FF and FcoR sequences back to the partial physical map of the *fuhc* locus, which consisted of seven scaffolds covering two *fuhc* haplotypes- (*fuhc* α and β ; Fig. 4a); isolated from California²⁵. In these haplotypes, we found that FF and FcoR loci are encoded head-to-head in pairs that correlated exactly with co-expression results from multiple individuals (FF1/FcoR7; FF3/FcoR1; FF22/FcoR42) (Fig. 4a, Extended Data Fig. 7, Table 3). In summary, the FF and FcoR genes are encoded in pairs in two haplotypes and also co-expressed in multiple wild-type individuals. Moreover, presence/absence polymorphism in haplotypes is of loci pairs.

Next, we analyzed the complete genome sequence of a single individual isolated from the Mediterranean coast of France³⁰. In this assembly, both haplotypes of each of the 16 chromosomes were recovered, allowing us to physically map the maternal and paternal chromosomes of this individual independently. Two FF/FcoR clusters are found in the genome, one within the *fuhc* locus on chromosome 11, and a separate cluster on chromosome 5 (Fig. 4b,c). The physical location of the FF and FcoR loci correlate exactly with the phylogenetic results- (Fig. 1,2) as intergenic recombination would be restricted to genes on the same chromosome. Moreover, despite the geographic distance, three of the FF/FcoR pairs found in individual transcriptomes from California are also encoded in the genome of the Mediterranean individual (FF1/FcoR7; FF12/FcoR3 and FF13/FcoR4), suggesting that the pairings are conserved, and this is notable as these are the three polymorphic pairs of genes (Fig. 4b,c and Extended Data Fig. 9, Table 3).

In addition, a third FcoR cluster is found on chromosome 9 (Fig. 4d). This region is also highly polymorphic, encoding over 13 FcoR genes over an ca. 1.2 Mb region. We detected presence/absence polymorphism between these two haplotypes, and this cluster is larger and more complex than those on the other two chromosomes. The presence of three FcoR clusters is also consistent with the phylogenetic analysis, which had split the FcoR sequences into clades that correspond with their chromosomal location (Fig. 1,2).

Next, we compared the sequenced genomic haplotypes of the *fuhc* on chromosome 11 (Fig. 4,5). This confirmed our previous results- the *fuhc* locus is embedded within two groups of conserved framework genes and consists of two parts. On one side, a 120Kb region encodes the candidate *fuhc* ligand genes: *bhf*, *fuhc-sec*, *fuhc-tm*, and *hsp40l*, (Fig. 4, 5A)¹⁷, which are conserved between individuals. In

contrast, the region spanning from *bhf* to *GMP synthase* genes encodes the highly divergent FF/FcoR haplotypes.

Comparison of the FF/FcoR cluster on chromosome 5 and the FcoR cluster on chromosome 9 tell the same story (Fig. 5b,c). The polymorphic receptor clusters are bounded by conserved framework genes, within which these receptors are evolving rapidly by birth and death evolution³¹, with little homology outside the genes themselves. Finally, both the genetic and physical mapping suggests that the majority of diversification is of the FF/FcoR pairs, but is not absolute, as transcriptomic analysis suggests there are cases where one partner is expressed alone (Extended Data Table 3).

Genotype specific expression of the FF and FcoR genes

In our initial studies we found genotype specific expression and alternative splice patterns of both FF1 and FF3, which we hypothesized were a result of a genotype specific calibration of these two signals that ensures specificity^{25,32}. We next surveyed expression patterns of the new FF and FcoR family members in ampullae isolated from different genotypes over multiple time points and found that the new loci were also differentially expressed in stable, genotype specific patterns, regardless of their chromosomal location (Extended Data Fig. 7, 8), consistent with our previous results.

Botryllus vasculature expresses orthologs of ITAM and ITIM signal transduction proteins

Finally, to determine if the cells involved in allorecognition co-express proteins involved in allorecognition and ITIM and ITAM signal transduction, we characterized gene expression in FACS isolated vascular cells^{32,33}. All candidate allorecognition genes in the *fuhc* locus were expressed in these cells, along with homologs of nearly every signal transduction protein used in ITAM and ITIM signaling in TCR and NK cells, as well as the transcription factors NFAT and NF κ B. Vascular cells also express multiple homologs of receptor-type protein phosphatases (Extended Data Fig. 10).

Interestingly, no ascidian genomes encode homologs of DAP12, DAP10, LAT or SLP-76 proteins^{30,34}. In summary, vascular cells express all allorecognition proteins as well as all signal transduction and most of the adaptors and transcription factors involved in ITAM and ITIM signaling in T- and NK cells.

Discussion

Allorecognition in *B. schlosseri* utilizes innate recognition mechanisms to discriminate between alleles of a highly polymorphic ligand. Natural populations have hundreds of transplantation specificities, which means this missing-self recognition system can pinpoint a self-allele from up to a thousand competing alleles. But how this level of specificity is achieved is not understood. In previous studies we had shown that, similar to NK cells, the allorecognition response in *Botryllus* was not a mutually exclusive outcome, but rather due to the integration of two independent signals, one generated by the binding of fester (FF1), and the other by the binding of uncle fester (FF3), and further that each signal could be manipulated *in vivo*^{25,26}. This suggested that the allorecognition response consisted of a species-specific initiation of a rejection response mediated by a non-polymorphic receptor, which could be overridden by recognition of a self-fuhc allele by a polymorphic receptor. While there were no signaling domains on either protein, we had already found that proteins encoding cytoplasmic ITIM and ITAM domains, as well as all associated signal transduction molecules used in mammals were present in ascidian and other invertebrate genomes^{16,34}, so hypothesized that signaling was via pairing with adaptor molecules containing the activating and inhibitory motifs.

Here we find that the fester locus is much more diverse than previously described, with over 37 loci encoded in diverse haplotypes on two chromosomes. These analyses also revealed the presence of an even more diverse gene family, the fester co-receptor (FcoR) genes. The FcoR are type I TM proteins that encode one or more intracellular tyrosine motifs, including canonical ITIM, hemITAM, and two types of tyrosine core motifs. Several also encode SH2 adaptor domains. The FcoR genes are even more diverse than the FF genes: thus far we have identified 53 FcoR loci, and these are encoded in clusters on three chromosomes. On two of those chromosomes (11 and 5) the FF and FcoR are encoded in pairs, while a third cluster on chromosome 9 encodes only FcoR genes (Fig. 4). These data show a diversity of innate receptors as well as linking the *Botryllus* allorecognition response to canonical immune signaling mechanisms.

While mammalian innate allorecognition receptors share a common polymorphic genomic organization and functional partitioning,^{13,18,35} the complexity of the *Botryllus* allorecognition system is unparalleled. The presence of two diverse gene families, their organization into pairs, and localization on multiple chromosomes are unique, and more in line with the increased specificity of *Botryllus* allorecognition. This redundancy may allow for both maintenance of some interactions via linkage to the fuhc ligand, while the unlinked clusters may allow for independent and rapid evolvability of those loci.

Allorecognition in *Botryllus* mediates the natural transplantation of germline stem cells between individuals³⁶. The transplant of stem cells is thought to be an altruistic interaction³⁷, but in some genotypes these stem cells can be parasitic, and once transplanted will replace the germline of the other individual³⁶. This is a strong selective force to diversify the fuhc locus, resulting in extraordinary

polymorphism that prevents parasitic genotypes from sweeping through a population³⁸. Diversification requires both changes in the ligand, and the ability to correctly detect those changes. Interestingly, the two sides of the locus are evolving using different mechanisms. The candidate ligand genes at the 3' region of the *fuhc* locus are linked in a conserved haplotype in all genotypes examined thus far, and diversifying by nucleotide substitutions and small intragenic exchanges^{39–41}. In contrast, the *fester* side at the 5' region is evolving by birth and death evolution of the loci driven mainly by duplication and recombination (Fig. 2)^{25,28}. We hypothesize that an upper limit on the discriminatory ability carried out by germline encoded proteins would restrain evolution of the ligand, resulting in different mechanisms diversifying each side of the locus.

If the birth and death evolution is a response to the selective pressure to co-evolve with a rapidly evolving ligand⁴², it was surprising to find that out of >35 *fester* and >50 *FcoR* newly identified loci, none are as highly polymorphic as FF1 or *FcoR7* (Extended Data Fig. 5). Previous results linked function to polymorphism: FF3 was monomorphic and responsible for species-specific activation, while the polymorphic FF1 was an inhibitory receptor discriminating *fuhc* polymorphisms^{25,26}. Results here are consistent- polymorphic FF are paired with polymorphic *FcoR* that encode an ITIM, while the non-polymorphic loci are also paired, and the partner *FcoR* encodes a hemITAM or core motif. In addition, comparing individual haplotypes from California and the Mediterranean show that presence/absence polymorphisms are of FF/*FcoR* pairs, suggesting that selection does not act on individual loci, but on specificity of the pair. Nevertheless, we would have predicted more polymorphism and inhibitory receptors.

What insight do these results give into the mechanisms underlying allorecognition? We had found that FF1 and FF3 were necessary and sufficient for fusion and rejection pathways, respectively- with one interesting exception (discussed below)^{25,26}. The reagents used in those studies did not cross react with new FF family members (Fig. 4a, Extended Data Fig. 2), suggesting that the FF/*FcoR* are either assembled into, or signal as, oligomers. Furthermore, our previous hypothesis of a single activating and inhibitory pathway was clearly oversimplified¹⁷. All full-length *FcoR* (but no FF) loci encode one or more tyrosine motifs (ITIM, ITSM, hemITAM, core motif), and some also encode SH2 domains. Many loci have combinations of motifs. In addition, both alleles and alternative splice variants of *FcoR3* and *FcoR4* swap signaling domains, which we hypothesize is important for specificity (Fig. 3; discussed below). While there is no known role of the core motif: YxxI/L/V^{43,44}, it could be part of either activating or inhibitory signaling. Alternatively, these motifs are equivalent to several of the phosphorylation sites on LAT and SLP-76, the two vertebrate signal transduction adaptors conspicuously absent in ascidians. This includes the presence of an acidic amino acid upstream of the tyrosine on half of them, a modification which has been shown to change the speed of phosphorylation, and plays a critical role in

polymorphic discrimination by the TCR⁴⁵. If allelic recognition is due to oligomerization of the FF and FcoR proteins at the cell/cell interface, some of these proteins may function as adaptors.

The presence of multiple loci coupled to a diversity of signaling motifs- including the potential to switch between putative activating, inhibitory or neutral functional roles, all indicate that complex tuning of ITAM and ITIM signaling may be required for allelic discrimination. We hypothesize this is due to an interplay of cooperative binding of oligomers that occur both in cis and trans⁴⁶⁻⁴⁸, with the end result is that ITAM/ITIM signals are integrated from multiple binding events, compared to an activation threshold, and the predominant signal determines outcome (fusion or rejection).

For both T- and NK-cells, effector specificity and function are not encoded in the genome. Both cells require a cell autonomous quality control process during development that takes randomly generated binding specificities and sets activation thresholds that allow a cell to be self-tolerant but functional^{4,9,10}. But how T- or NK cells establish these thresholds remains unclear. Similarly, specificity in *Botryllus* does not appear to be hardwired: the extreme polymorphism rules out a simple lock and key interaction between complementary genes, and this mechanism is inconsistent with the genetics of the locus¹⁷, and results presented here. We hypothesize that specificity is due to an education process which would modify the stoichiometry of the oligomers until specificity was achieved, reminiscent of the rheostat model of NK education, but with more influence by polymorphisms of the histocompatibility ligand^{49,50}. This is consistent with findings that genotype specific expression and alternative splicing patterns of FF1 and FF3 are maintained following multiple cycles of ablation and regeneration of the ampullae (Extended Data Fig. 7,8)^{25,32}.

In mammals, education is a conserved process required for effector function in five unrelated receptor/ligand pairs: KIR-MHC Class 1; Ly49-MHC Class I; CD94/NKG2-HLA E (Qa-1); Nkrp1-clr-b; and Sirp α -CD47. Each uses a missing-self strategy to determine the health of target cells, and in each knockout of the inhibitory ligand (MHC Class I; Clr-b; or CD47), which would predict an autoimmune phenotype, does exactly the opposite- resulting in tolerance^{62,63,64,65}. In addition, in NK cells it has been demonstrated that this tolerance is reversible- NK cells that develop in an MHC deficient background are anergic, but regain functionality after being transplanted into a wild-type background, and wild-type NK cells can acquire tolerance when transplanted into a MHC deficient background^{51,52}. Similarly, knockout of the inhibitory receptor *FF1* blocked both fusion and rejection responses from occurring¹⁶. We had originally hypothesized that FF1 might be a subunit of both activating and inhibitory receptors²⁵. However, in retrospect this could also be revealing an evolutionarily conserved characteristic of ITIM/ITAM signal transduction- constant inhibitory signaling is required for maintenance of effector function in mature cells. This dynamic tuning is also present in T-cells⁵³, and may have clinical consequences on the long-term efficacy of checkpoint therapy.

In summary, our findings suggest that the mechanisms that underlie polymorphic discrimination rely on the dynamic range provided by the interaction between ITAM and ITIM signaling pathways. Both thymic and NK education take receptor diversity and create specificity^{4,9,10}, and a similar process existed long before the emergence of vertebrates. Conservation of tunable signal transduction pathways allow receptors to evolve freely, and can explain the rapid, recurrent and convergent evolution of missing self-recognition systems^{13,18,35}, as well as the emergence of adaptive immunity¹². The results of this study coupled to the unique characteristics of Botryllus allorecognition²⁰ provide a potent model to study these fundamental mechanisms.

Acknowledgments

We thank Greg Stoney for collecting and maintain the animals used here, and the Center for Scientific Computing (CSC) of the University of California, Santa Barbara for sharing its clusters to perform the bioinformatics analysis. This research was supported by the NIH grants GM139649 and OD030520 to AWD, and the ANR (ANR-14-CE02-0019-01) and INSB-DBM EVOCHORE to ST.

Author Contributions

HRV and AWD conceived the project and wrote the manuscript. JS assisted HRV with genetic analyses, ST, ODT and FF provided genomic, technical and scientific insights. AWD supervised the research. All authors edited the manuscript and approved the final version.

Competing Interests: The authors have no competing interests.

Materials and methods

Animal collection and maintenance

B. schlosseri individuals were collected in the Santa Barbara Harbor (CA, US, 34°24'11"N 119°41'31"W). Animals were maintained with seawater flow at 18C and fed with different species of algae (*Nannochloropsis* sp., *Tetraselmis* sp., *Isochrysis* sp., *Dunaliella salina*) (Carolina Biological Supply, US) two times per day as described previously⁵⁴.

Identification of *fester* and *FcoR* genes

We used the *fester* (DQ517888.1) and *uncle feater* (JF806283.1) genes of *B. schlosseri* as queries to tBLASTx search in different *B. schlosseri* transcriptomes publicly available or previously sequenced in our laboratory (Extended Data Table 1). Raw reads were cleaned of adaptors and low-quality sequences with Trim Galore software using the default parameters (<https://github.com/FelixKrueger/TrimGalore>). Transcriptome assemblies were performed with the Trinity software using the default parameters⁵⁵. Raw reads were deposited in the GenBank under the accession numbers ####. Assembled transcriptomes and gene alignments were deposited on GitHub. To identify *FcoR* genes, the *fester* genes from *B. schlosseri* were initially used as queries in a search (tBLASTx) in the transcriptomes and genomes of this species. Finally, identified *FcoR* genes were used as queries in a search (tBLASTx) for additional *FcoR* genes in the databases of this species. Alignments were performed using the BioEdit software⁵⁶.

Quantification of *fester* and *FcoR* genes

To quantify the expression of *fester* and *FcoR* genes, raw reads from *B. schlosseri* transcriptomes were mapped to the full-length of *fester* and *FcoR* genes using the kallisto method⁵⁷. Trimmed Mean of M-values (TMM) were used to quantify the expression of *fester* and *FcoR* genes. To estimate the number of *fester* and *FcoR* genes per individual, an average was made between the number of *fester* genes present in the replicates corresponding to each individual.

Identity matrices of *fester* and *FcoR* genes and loci/allele predictions

Multiple alignments of *fester* and *FcoR* genes were performed with ClustalW and identity matrices were generated with the BioEdit software⁵⁶. Data visualization was performed with ggplot2 in RStudio (<https://posit.co/>). To predict which sequences represented unique loci vs alleles, we used amino acid and nucleotide identity values from the most divergent alleles identified in a previous population genetic study of *fester* as a metric, which analyzed >60 alleles found in populations from both the East and

West Coast of the U.S.²⁸. We identified sequences that had > 80% identity at the amino acid level (Extended Data Fig. 1). If those sequences also shared >90% nucleotide identity over the entire gene sequence, we classified these as alleles. This seemed to be a conservative threshold for both *FF* and *FcoR*, as the only sequences that had nucleotide alignment over their entire length were >90% identical. No other pairs of sequences had homology over the entire length.

Amplification of *fester* genes from genomic DNA and mRNA

fester genes of *B. schlosseri* were amplified from genomic DNA and mRNA. mRNA sequences of *B. schlosseri fester* genes were aligned with the BioEdit software⁵⁶, and primers were designed for each *fester* gene. For genomic amplification, the size of the amplified regions was between 100 and 200 bp, which sought the amplification of genomic fragments belonging to single exons. Meanwhile, primers covering the full-length of the *fester* genes (approximately 1000 bp) were designed for amplification from mRNA. A full list of primers used in this study is provided in Extended Data Table 2. Genomic DNA was isolated from whole colonies of *B. schlosseri* with the NucleoSpin Tissue, Mini kit for DNA from cells and tissue (Macherey-Nagel) following the manufacturer's protocol. Meanwhile, total RNA was isolated for the same individuals with the Monarch® Total RNA Miniprep Kit (New England Biolabs) following the manufacturer's protocol. cDNA was synthesized by adding 200units M-MuLV Reverse Transcriptase, 1X M-MuLV Reverse Transcriptase Reaction Buffer (New England Biolabs), 5mM DTT, 40U RNaseOUT (Thermo Fisher), incubating at 42°C for 1h, and at 70°C for 15 minutes. Gene amplification was performed with the Classic Taq DNA Polymerase Master Mix (Tonbo Biosciences) and 0.5uM of each primer. Amplification protocol consisted of an initial denaturation at 95°C for 2 minutes and 30 seconds, a second denaturation at 95°C for 20 seconds, an annealing step at 57°C for 20 sec and an elongation step at 72°C for 20 sec, repeating these last three steps 35 times, and a final elongation step at 72°C for 5 minutes. PCR products were analyzed by gel electrophoresis.

Genomic annotation of *fester* and *FcoR* genes

fester and *FcoR* transcriptomic sequences were used as queries (tBLASTx) to identify the genomic scaffolds of *B. schlosseri* containing these genes. Genomic scaffolds were obtained from²⁵ and a draft genome of *B. schlosseri*³⁰. Transcripts sequences were then manually aligned with the genomic scaffolds to establish the exon-intron boundaries of the *fester* and *FcoR* genes. Genomic scaffolds were annotated with the GenScan software (<http://hollywood.mit.edu/GENSCAN.html>)⁵⁸ and BLASTp using the non-redundant protein sequences (nr). Additionally, tyrosine-based motifs (SH2 motifs) of *FcoR* proteins were predicted with the Scansite 4.0 software (<https://scansite4.mit.edu/#home>)⁵⁹, or manually annotated following reported sequences of ITIM ([S/I/V/L]xYxx[I/V/L]; where x represents any

amino acid, hemITAM (three acidic amino acids [D/E] follow by xYxxL), ITSM ([S/T]xYxx[L/I]), and two 'core' tyrosine-based (Yxx[L/V/I]; [V/I]Yxx[V/L]) motifs²⁹.

Linkage analysis between *fester* genes and the *fuhc* locus

fester genes were amplified from genomic DNA of *fuhc* scored F₂ and backcross progeny from defined crosses using five *fuhc* haplotypes (α , β , X, C, D)²⁵. The PCR amplification protocol from genomic DNA was the same as that described above. Primers are provided in Extended Data Table 2. PCR products were analyzed by gel electrophoresis.

Phylogenetic analysis of *fester* and *FcoR* genes

Alignments of the full-length *fester* and *FcoR* proteins of *B. schlosseri* were performed with Muscle software (<https://www.ebi.ac.uk/Tools/msa/muscle/>)⁶⁰. Phylogenetic trees were generated by the Maximum likelihood method with 10000 bootstrap replicates using the IQ-TREE web server (<http://iqtree.cibiv.univie.ac.at/>)⁶¹, and edited with the iTOL software (<https://itol.embl.de/upload.cgi>)⁶². Additionally, phylogenetic trees with the extracellular and transmembrane/cytoplasmic regions of the *fester* and *FcoR* proteins were generated using the same strategy described above. Transmembrane domains of the *fester* and *FcoR* proteins were predicted with InterProScan software (<https://www.ebi.ac.uk/interpro/search/sequence/>)⁶³.

Comparison of genomic regions with *fester* and *FcoR* genes

Genomic regions with *fester* and *FcoR* genes were *in silico* isolated from two different haplotypes (h1 and h2) of *B. schlosseri*. These genomic regions from chromosomes 5, 9 and 11 were pairwise aligned using Emboss stretcher⁶⁴. Dot plots were generated using Geneious Prime.

Polymorphism of *fester* and *FcoR* genes

Amino acid diversity of *fester* and *FcoR* genes was calculated using the diversity value (d)^{62,65}. *BsFesterCo7* sequences were isolated from different *B. schlosseri* transcriptomes. *FF1* sequences were previously reported²⁸. Alignments were performed using the BioEdit software⁵⁶. Redundant sequences were removed before diversity values were calculated. Amino acid positions with 100% conservation (diversity value=0.05) were excluded in the visualization of the results.

Identification of NK-cell gene homologs

Human ITAM and ITIM signal transduction proteins were collected from the KEGG database (<https://www.genome.jp/kegg/>), and used as queries (tBLASTx) to search a publicly available

transcriptome database of *B. schlosseri* (<http://octopus.obs-vlfr.fr/>). Putative homologs were annotated with BLASTp and InterProscan software to determine the identity and domain architecture of these proteins. Expression was characterized in FACS isolated vascular cells as described¹⁸. *Botryllus* homologs were deposited in GenBank.

References

1. Snell, G. D. Studies in histocompatibility. *Science* 172–178 (1981).
2. Kärre, K. Natural killer cell recognition of missing self. *Nat. Immunol.* **9**, 477–480 (2008).
3. Sibener, L. V. *et al.* Isolation of a Structural Mechanism for Uncoupling T Cell Receptor Signaling from Peptide-MHC Binding. *Cell* **174**, 672–687.e27 (2018).
4. Ashby, K. M. & Hogquist, K. A. A guide to thymic selection of T cells. *Nat. Rev. Immunol.* **24**, 103–117 (2024).
5. Lanier, L. L. NK Cell Recognition. *Annu Rev Immunol* **23**, 225–274 (2005).
6. Štefanová, I. *et al.* TCR ligand discrimination is enforced by competing ERK positive and SHP-1 negative feedback pathways. *Nat Immunol* **4**, 248–254 (2003).
7. Stebbins, C. C. *et al.* Vav1 Dephosphorylation by the Tyrosine Phosphatase SHP-1 as a Mechanism for Inhibition of Cellular Cytotoxicity. *Mol. Cell. Biol.* **23**, 6291–6299 (2003).
8. Hui, E. & Vale, R. D. In vitro membrane reconstitution of the T-cell receptor proximal signaling network. *Nat. Struct. Mol. Biol.* **21**, 133–142 (2014).
9. Joncker, N. T., Fernandez, N. C., Treiner, E., Vivier, E. & Raullet, D. H. NK Cell Responsiveness Is Tuned Commensurate with the Number of Inhibitory Receptors for Self-MHC Class I: The Rheostat Model. *J Immunol* **182**, 4572–4580 (2009).
10. Brodin, P., Kärre, K. & Höglund, P. NK cell education: not an on-off switch but a tunable rheostat. *Trends Immunol.* **30**, 143–149 (2009).
11. Scofield, V. L., Schlumpberger, J. M., West, L. A. & Weissman, I. L. Protochordate allorecognition is controlled by a MHC-like gene system. *Nature* **295**, 499–502 (1982).
12. Flajnik, M. F. & Kasahara, M. Origin and evolution of the adaptive immune system: genetic events and selective pressures. *Nat Rev Genet* **11**, 47–59 (2010).
13. Parham, P. Co-evolution of lymphocyte receptors with MHC class I. *Immunol Rev* **267**, 1–5 (2015).
14. Weisel, D. J. *et al.* A highly diverse set of novel immunoglobulin-like transcript (NILT) genes in zebrafish indicates a wide range of functions with complex relationships to mammalian receptors. *Immunogenetics* 1–17 (2022) doi:10.1007/s00251-022-01270-9.
15. Grice, L. F. *et al.* Origin and Evolution of the Sponge Aggregation Factor Gene Family. *Mol Biol Evol* **34**, 1083–1099 (2017).
16. Nicotra, M. L. Invertebrate allorecognition. *Curr Biol* **29**, R463–R467 (2019).
17. Taketa, D. A. & De Tomaso, A. W. Botryllus schlosseri allorecognition: tackling the enigma. *Dev Comp Immunol* **48**, 254–265 (2015).
18. Kelley, J., Walter, L. & Trowsdale, J. Comparative Genomics of Natural Killer Cell Receptor Gene Clusters. *Plos Genet* **1**, e27 (2005).
19. Huene, A. L. *et al.* A family of unusual immunoglobulin superfamily genes in an invertebrate histocompatibility complex. *Proc. Natl. Acad. Sci.* **119**, e2207374119 (2022).
20. De Tomaso, A. W. Sea squirts and immune tolerance. *Dis Model Mech* **2**, 440–445 (2009).
21. Delsuc, F., Brinkmann, H., Chourrout, D. & Philippe, H. Tunicates and not cephalochordates are the closest living relatives of vertebrates. *Nature* **439**, 965–968 (2006).
22. Sabbadin, A. Le basi genetiche della capacita di fusione fra colonies in Botryllus schlosseri (Asidiacea). *Rend Accad Naz Lincie, Series* **8 32**, 1031–1035 (1962).

23. Rinkevich, B., Porat, R. & Goren, M. Allorecognition elements on a urochordate histocompatibility locus indicate unprecedented extensive polymorphism. *Proc. R. Soc. Lond. Ser. B: Biol. Sci.* **259**, 319–324 (1995).
24. Grosberg, R. K. & Quinn, J. F. The genetic control and consequences of kin recognition by the larvae of a colonial marine invertebrate. *Nature* **322**, 456–459 (1986).
25. Nyholm, S. V. *et al.* fester, a Candidate Allorecognition Receptor from a Primitive Chordate. *Immunity* **25**, 163–173 (2006).
26. McKittrick, T. R., Muscat, C. C., Pierce, J. D., Bhattacharya, D. & De Tomaso, A. W. Allorecognition in a Basal Chordate Consists of Independent Activating and Inhibitory Pathways. *Immunity* **34**, 616–626 (2011).
27. Blanchoud, S., Rutherford, K., Zondag, L., Gemmell, N. J. & Wilson, M. J. De novo draft assembly of the Botrylloides leachii genome provides further insight into tunicate evolution. *Sci Rep-uk* **8**, 5518 (2018).
28. Nydam, M. L. & De Tomaso, A. W. The fester locus in Botryllus schlosseri experiences selection. *BMC Evol. Biol.* **12**, 249 (2012).
29. Bauer, B. & Steinle, A. HemITAM: A single tyrosine motif that packs a punch. *Sci. Signal* **10**, eaan3676, (2017).
30. Thier, O. D. *et al.* First chromosome-level genome assembly of the colonial tunicate Botryllus schlosseri. *bioRxiv* 2024.05.29.594498 (2024) doi:10.1101/2024.05.29.594498.
31. Nei, M., Gu, X. & Sitnikova, T. Evolution by the birth-and-death process in multigene families of the vertebrate immune system. *Proc. Natl. Acad. Sci. U. S. A.* **94**, 7799–7806 (1997).
32. Taketa, D. A., Cengher, L., Rodriguez, D., Langenbacher, A. D. & De Tomaso, A. W. Genotype-specific expression of uncle fester suggests a role in allorecognition education in a basal chordate. *Integrative and Comparative Biology* **icae107**, (2024).
33. Rodriguez, D. *et al.* In vivo manipulation of the extracellular matrix induces vascular regression in a basal chordate. *Mol Biol Cell* **28**, 1883–1893 (2017).
34. Azumi, K. *et al.* Genomic analysis of immunity in a Urochordate and the emergence of the vertebrate immune system: “waiting for Godot.” *Immunogenetics* **55**, 570–581 (2003).
35. Carlyle, J. R. *et al.* Evolution of the Ly49 and Nkrp1 recognition systems. *Semin Immunol* **20**, 321–330 (2008).
36. Sabbadin, A. & Zaniolo, G. Sexual differentiation and germ cell transfer in the colonial ascidian Botryllus schlosseri. *J Exp Zool* **207**, 289–304 (1979).
37. De Tomaso, A. W. Allorecognition polymorphism versus parasitic stem cells. *Trends Genet* **22**, 485–490 (2006).
38. Buss, L. W. Somatic cell parasitism and the evolution of somatic tissue compatibility. *Proc. Natl. Acad. Sci.* **79**, 5337–5341 (1982).
39. Nydam, M. L., Taylor, A. A. & De Tomaso, A. W. Evidence for selection on a protochordate histocompatibility locus. *Evolution* **67**, 487–500 (2013).
40. Nydam, M. L., Hoang, T. A., Shanley, K. M. & De Tomaso, A. W. Molecular evolution of a polymorphic HSP40-like protein encoded in the histocompatibility locus of an invertebrate chordate. *Dev Comp Immunol* **41**, 128–136 (2013).
41. Taketa, D. A. *et al.* Molecular evolution and in vitro characterization of Botryllus histocompatibility factor. *Immunogenetics* **67**, 605–623 (2015).
42. Nei, M., Gu, X. & Sitnikova, T. Evolution by the birth-and-death process in multigene families of the vertebrate immune system. *Proc National Acad Sci* **94**, 7799–7806 (1997).
43. Hughes, C. E. *et al.* Critical Role for an Acidic Amino Acid Region in Platelet Signaling by the HemITAM (Hemi-immunoreceptor Tyrosine-based Activation Motif) Containing Receptor CLEC-2 (C-type Lectin Receptor-2)*. *J. Biol. Chem.* **288**, 5127–5135 (2013).
44. Bauer, B. & Steinle, A. HemITAM: A single tyrosine motif that packs a punch. *Sci. Signal.* **10**, (2017).

45. Lo, W.-L. *et al.* A single-amino acid substitution in the adaptor LAT accelerates TCR proofreading kinetics and alters T-cell selection, maintenance and function. *Nat Immunol* **24**, 676–689 (2023).
46. Held, W. & Mariuzza, R. A. Cis–trans interactions of cell surface receptors: biological roles and structural basis. *Cell. Mol. Life Sci.* **68**, 3469 (2011).
47. Stengel, K. F. *et al.* Structure of TIGIT immunoreceptor bound to poliovirus receptor reveals a cell–cell adhesion and signaling mechanism that requires cis-trans receptor clustering. *Proc. Natl. Acad. Sci.* **109**, 5399–5404 (2012).
48. Goodman, K. M. *et al.* How clustered protocadherin binding specificity is tuned for neuronal self-/nonself-recognition. *eLife* **11**, e72416 (2022).
49. Sternberg-Simon, M. *et al.* Natural Killer Cell Inhibitory Receptor Expression in Humans and Mice: A Closer Look. *Front Immunol* **4**, 65 (2013).
50. Shilling, H. G. *et al.* Genetic Control of Human NK Cell Repertoire. *J Immunol* **169**, 239–247 (2002).
51. Elliott, J. M., Wahle, J. A. & Yokoyama, W. M. MHC class I–deficient natural killer cells acquire a licensed phenotype after transfer into an MHC class I–sufficient environment. *J Exp Medicine* **207**, 2073–2079 (2010).
52. Joncker, N. T., Shifrin, N., Delebecque, F. & Raulet, D. H. Mature natural killer cells reset their responsiveness when exposed to an altered MHC environment. *J Exp Medicine* **207**, 2065–2072 (2010).
53. Grossman, Z. & Paul, W. E. Adaptive cellular interactions in the immune system: the tunable activation threshold and the significance of subthreshold responses. *Proc. Natl. Acad. Sci.* **89**, 10365–10369 (1992).
54. Boyd, H. C., Brown, S. K., Harp, J. A. & Weissman, I. L. Growth and sexual maturity of laboratory-cultured Monterey Botryllus schlosseri. *Biol. Bull.* **170**, 91–109 (1986).
55. Grabherr, M. G. *et al.* Full-length transcriptome assembly from RNA-Seq data without a reference genome. *Nature Biotechnology* **29**, 644–652 (2011).
56. Hall & T., A. BioEdit: a user-friendly biological sequence alignment editor and analysis program for Windows 95/98/NT. *Nucleic Acids Symposium Series* **41**, 95–98 (1999).
57. Dillies, M.-A. *et al.* A comprehensive evaluation of normalization methods for Illumina high-throughput RNA sequencing data analysis. *Briefings in Bioinformatics* **14**, 671–683 (2013).
58. Burge, C. & Karlin, S. Prediction of complete gene structures in human genomic DNA. *Journal of Molecular Biology* **268**, 78–94 (1997).
59. Obenaus, J. C., Cantley, L. C. & Yaffe, M. B. Scansite 2.0: Proteome-wide prediction of cell signalling interactions using short sequence motifs. *Nucleic Acids Research* **31**, 3635–3641 (2003).
60. Edgar & R., C. MUSCLE: multiple sequence alignment with high accuracy and high throughput. *Nucleic acids research* **32**, 1792–7 (2004).
61. Trifinopoulos, J., Nguyen, L., Haeseler, A. V. & Minh, B. Q. W-IQ-TREE : a fast online phylogenetic tool for maximum likelihood analysis. **44**, 232–235 (2016).
62. Letunic, I. & Bork, P. Interactive Tree Of Life (iTOL) v5: an online tool for phylogenetic tree display and annotation. *Nucleic Acids Research* **49**, W293–W296 (2021).
63. Jones, P. *et al.* InterProScan 5: Genome-scale protein function classification. *Bioinformatics* **30**, 1236–1240 (2014).
64. Madeira, F. *et al.* The EMBL-EBI Job Dispatcher sequence analysis tools framework in 2024. *Nucleic Acids Research* **gkae241**, (2024).

65. Rodi, D. J., Mandava, S. & Makowski, L. DIVAA: analysis of amino acid diversity in multiple aligned protein sequences. *Bioinformatics* **20**, 3481–3489 (2004).

Figures and Tables

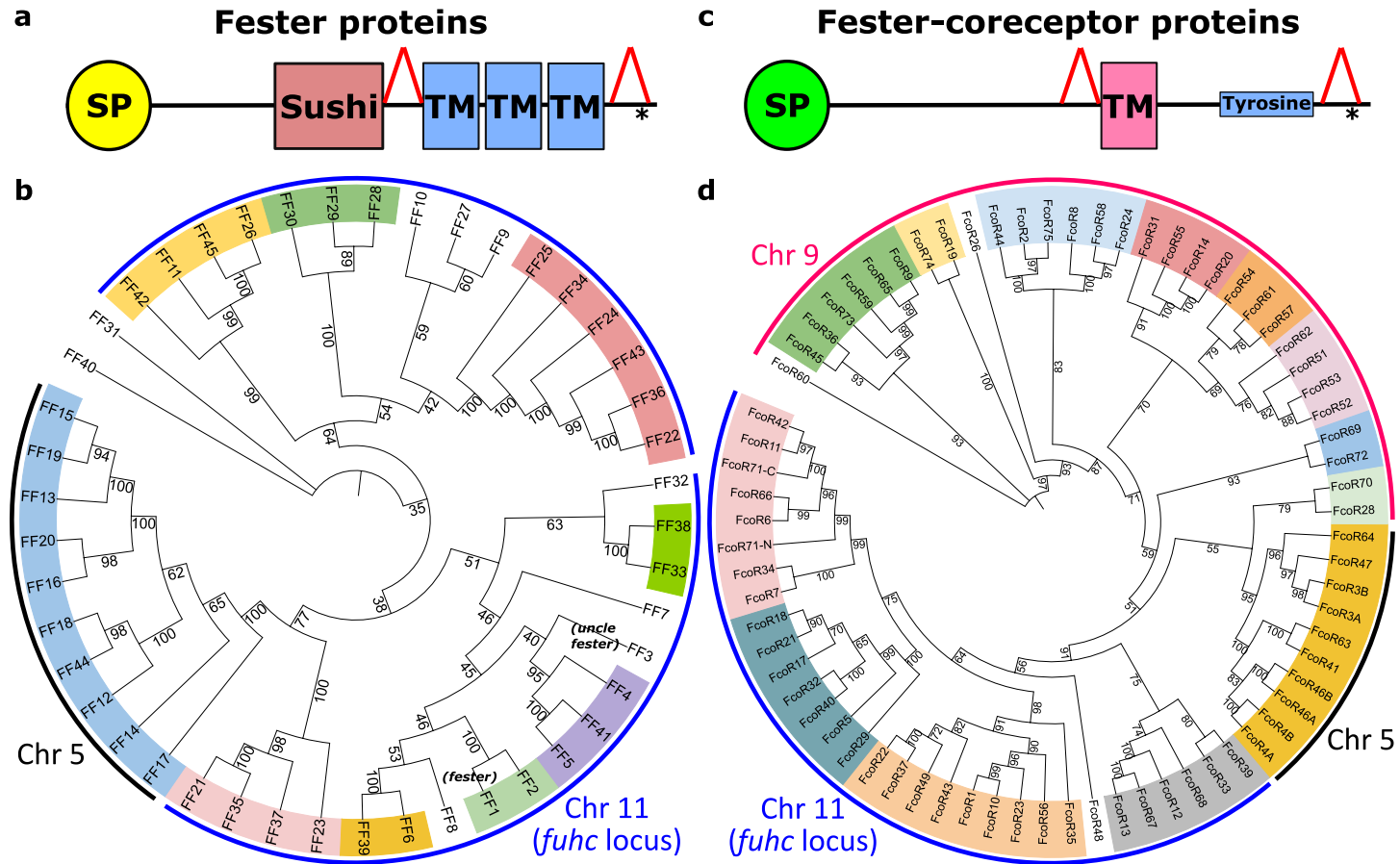
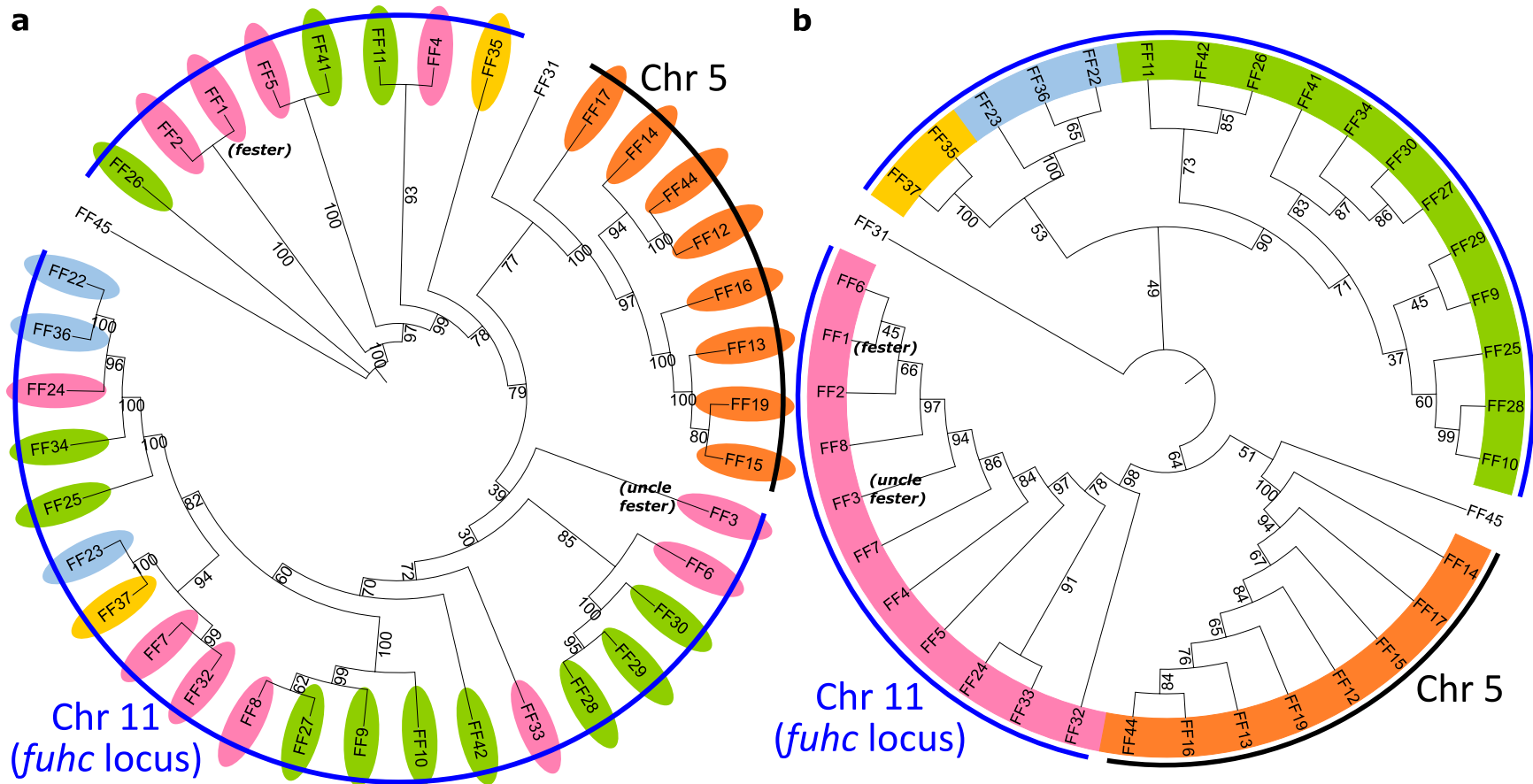


Fig. 1 Phylogenetic analysis of full-length Fester and FcoR proteins. a,c Illustration of domain architectures and b,d phylogenetic trees of the full-length fester (n=45) and FcoR proteins (n=69) performed using Maximum likelihood method. Bootstrap supports are indicated at the base of the branches. Well-supported clades are highlighted in different colors. *FF1* (*fester*) and *FF3* (*uncle fester*) genes are indicated. Putative chromosomal localizations are indicated (Fig. 4). Red triangles in a,c illustrate regions that are alternatively spliced.



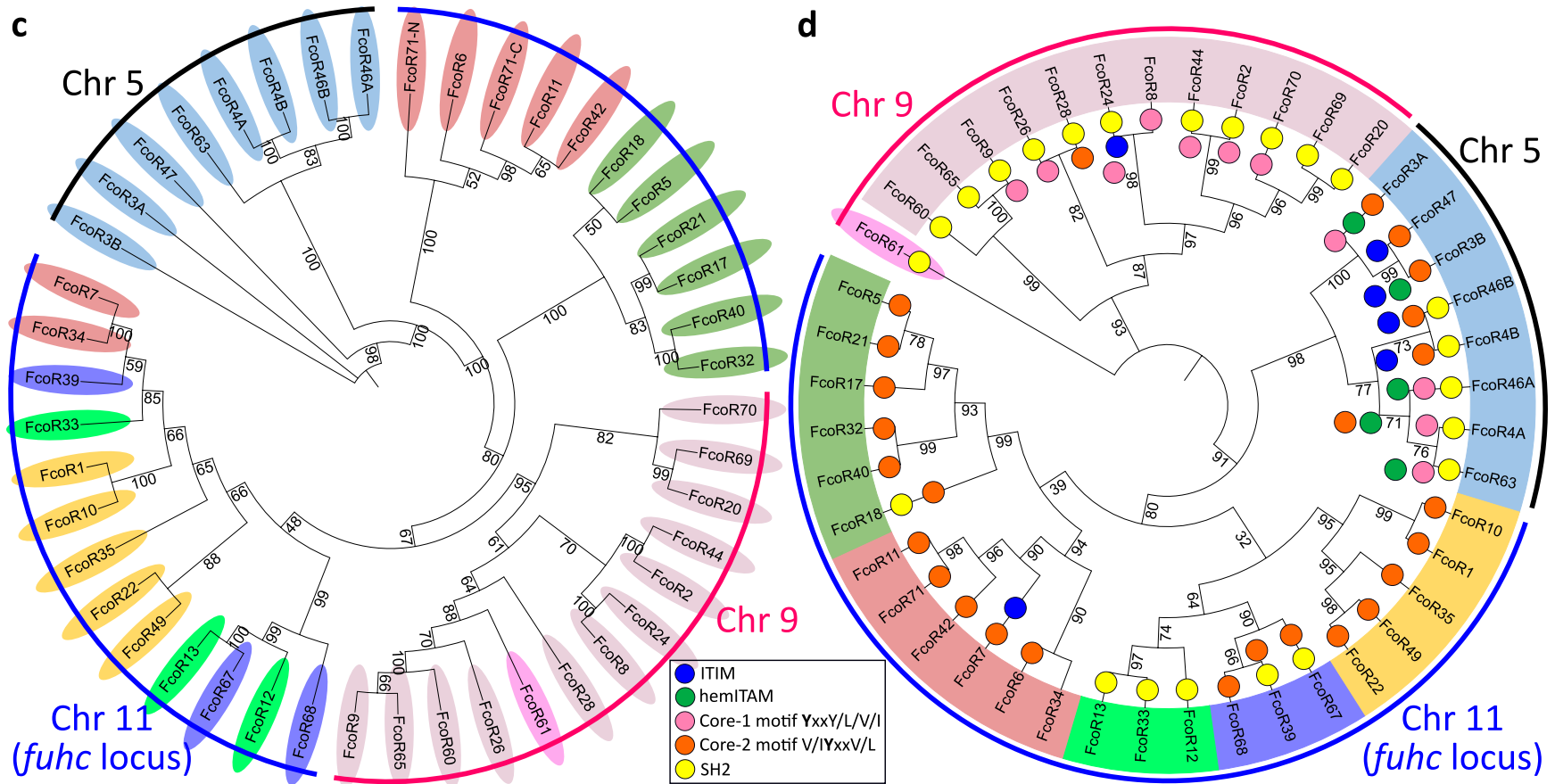


Fig. 2 Phylogenetic trees of extracellular and intracellular regions of FF and FcoR proteins. **a**, Phylogenetic trees of the extracellular and **b**, intracellular regions of Fester proteins (n=38). **c**, Phylogenetic trees of the extracellular and **d**, intracellular regions of FcoR (n=44). Bootstrap supports are indicated at the base of the branches. Clades were highlighted based on their similarity in the intracellular regions. Tyrosine-based motifs for FcoR proteins are indicated (colored circles).

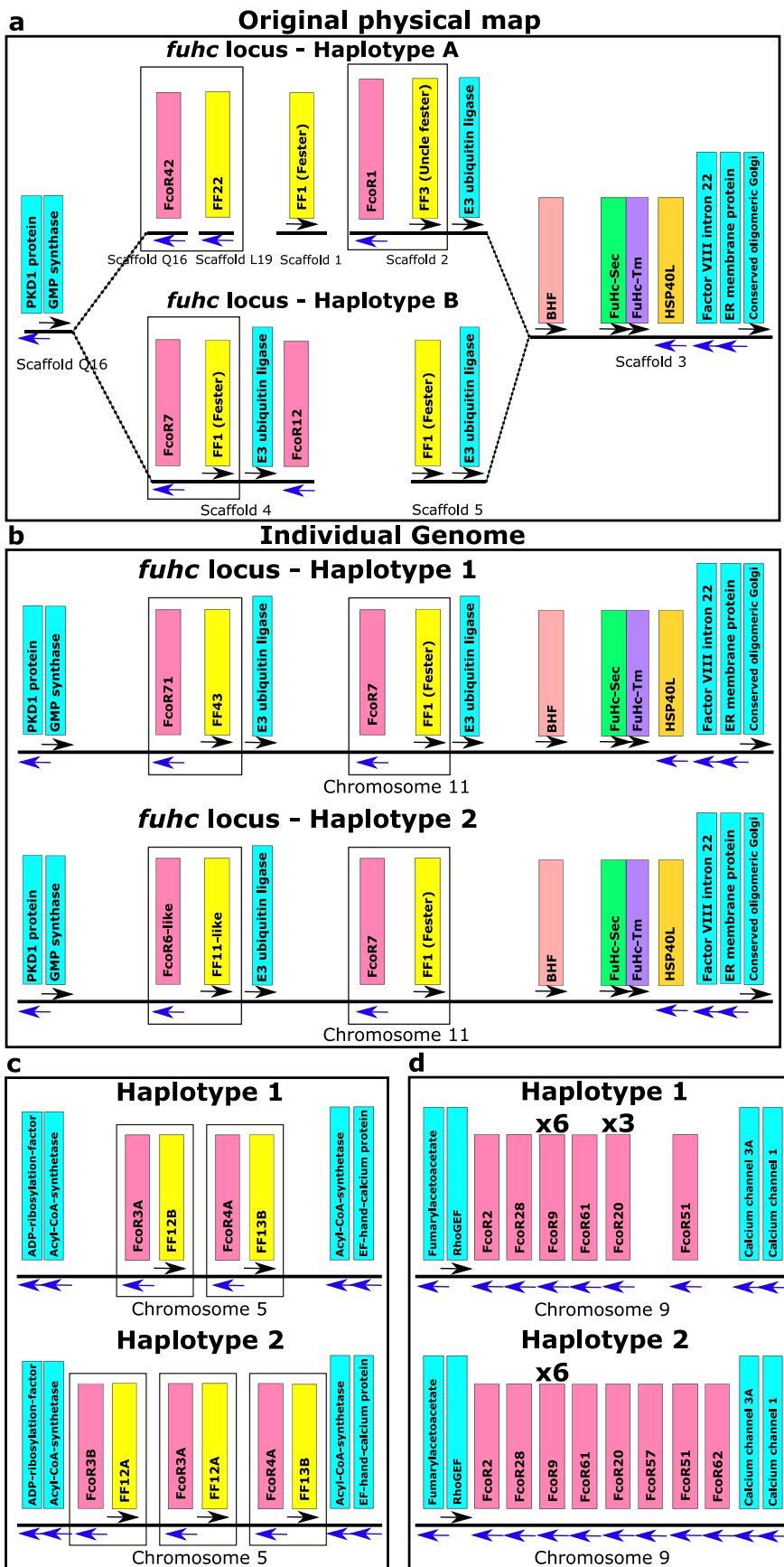
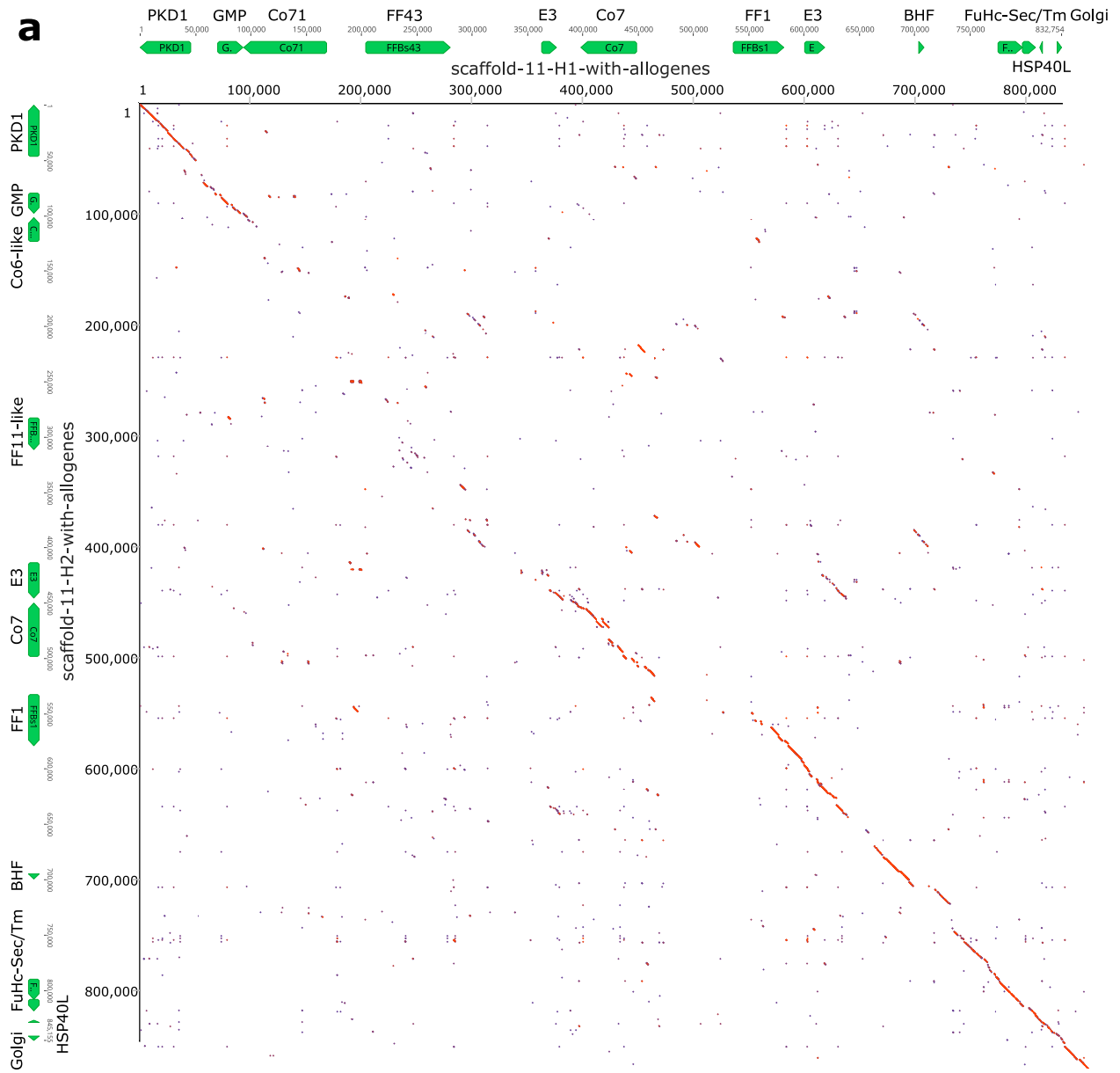
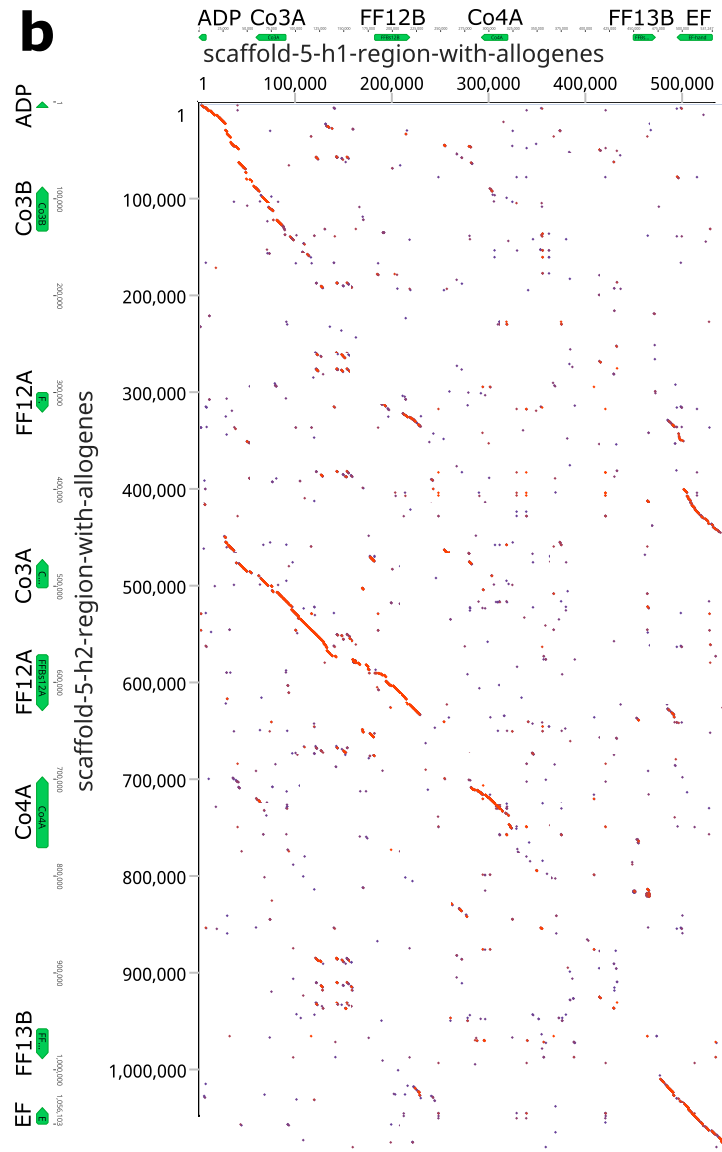


Fig. 4 Haplotypic variation of *fester* and *FcoR* genes. **a**, Partial physical maps of the α and β haplotypes of the *fhc* locus from individuals in California **b**, Comparison of the maternal and paternal haplotype of the *fhc* locus (Chromosome 11) from a single individual from the Mediterranean. **c**, Comparison of two haplotypes encoding FF/*FcoR* pairs on chromosome 5 from the same individual. **d**, Comparison of two haplotypes of the *FcoR* cluster found on chromosome 9. *fester* and *FcoR* genes are highlighted in yellow and pink, respectively. Framework genes are highlighted in blue.





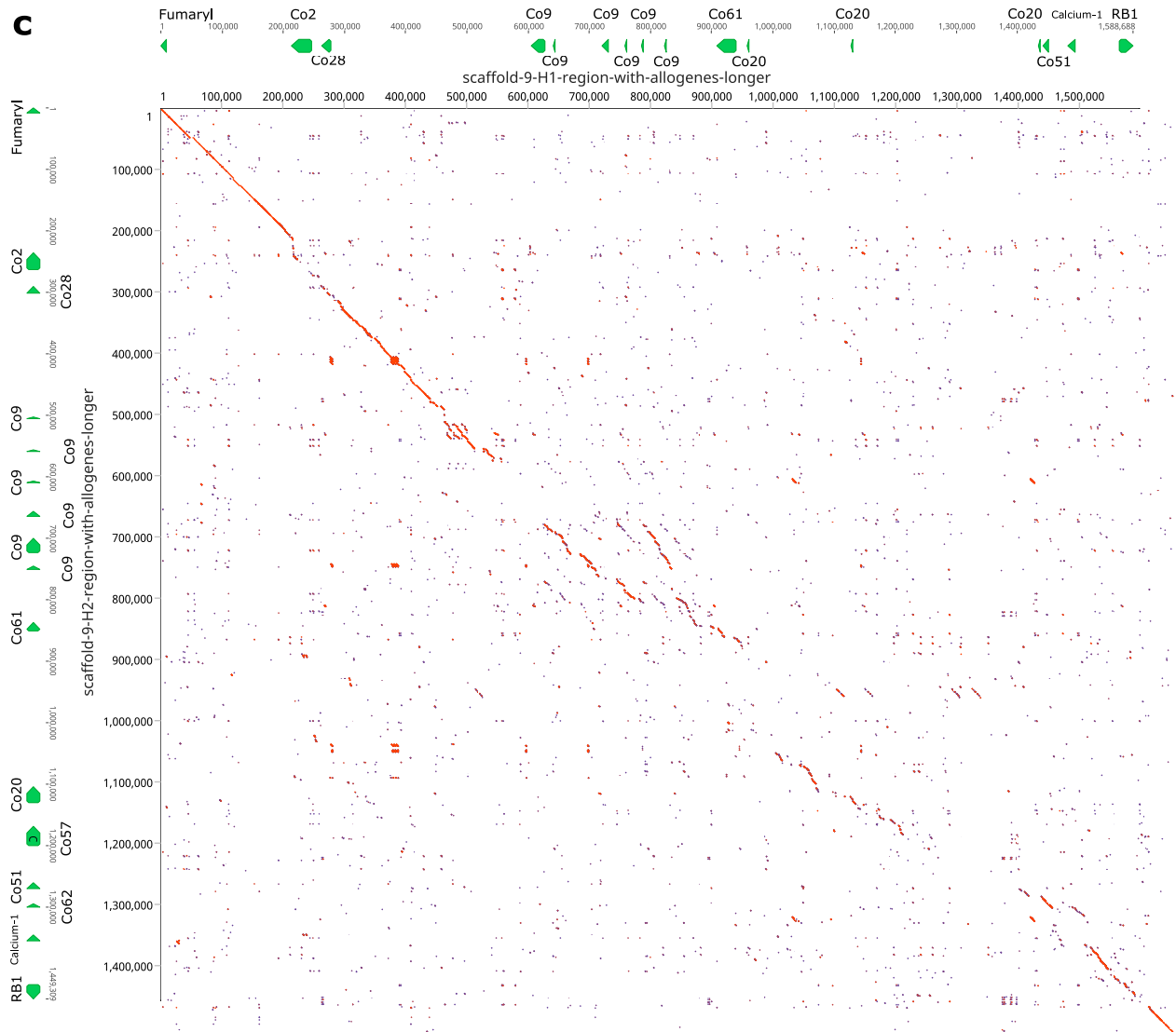
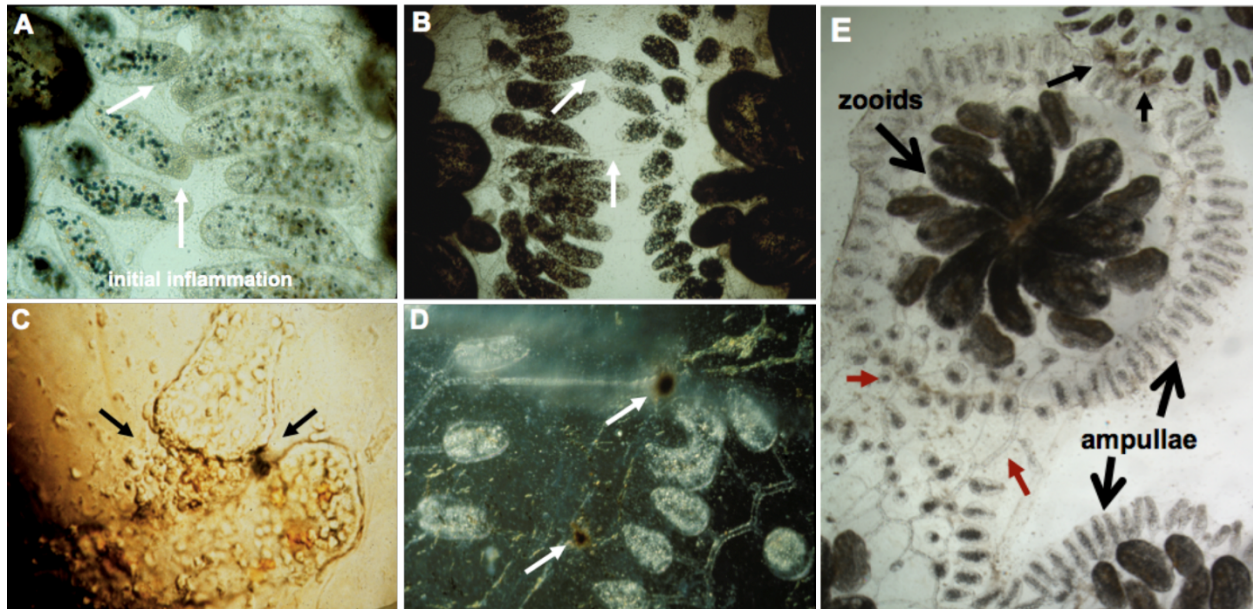
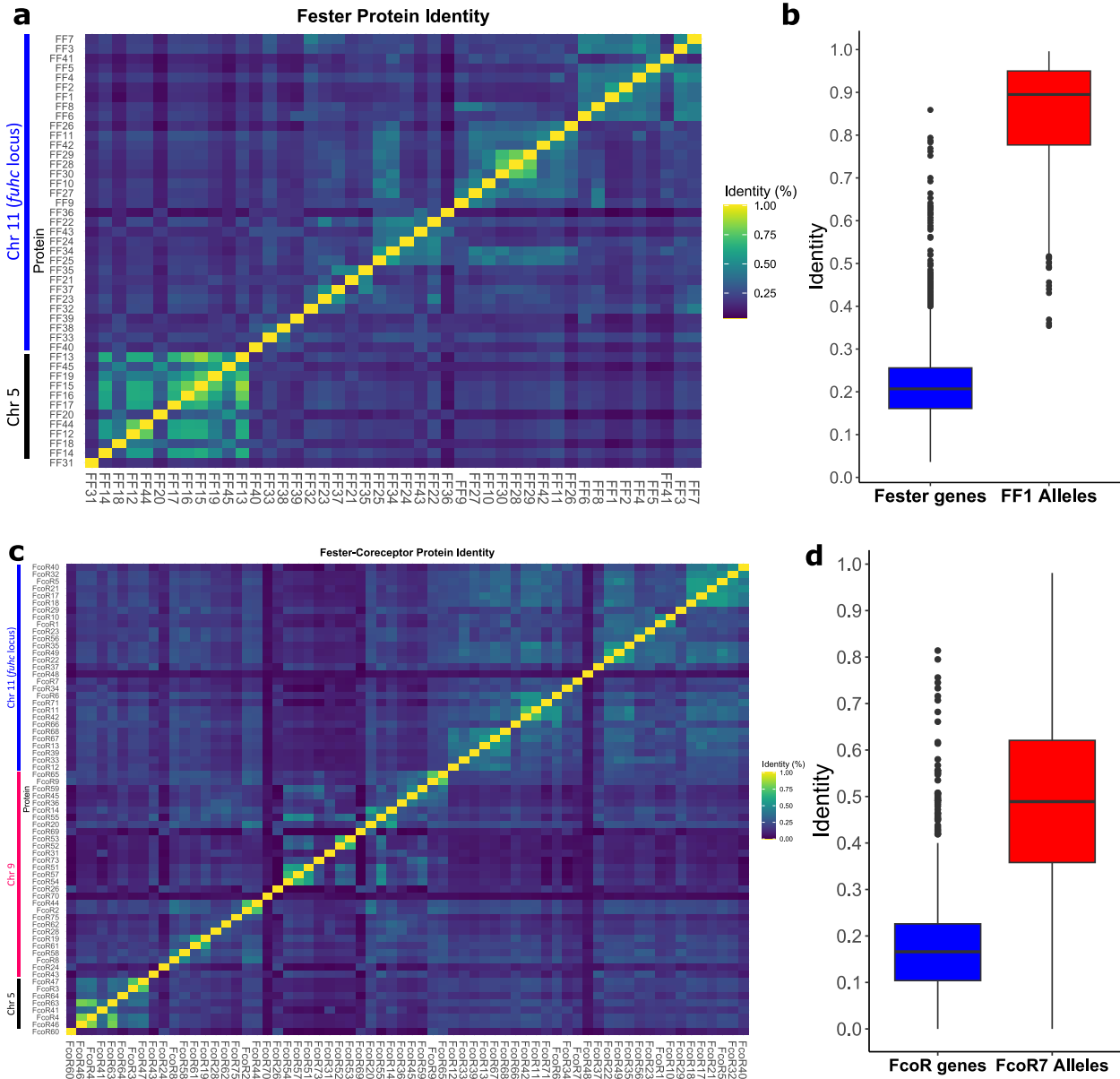


Fig. 5 Comparison of maternal and paternal haplotypes at the three allorecognition loci. Dot plot comparison of the two haplotypes from **a**, Chromosome 11. **b**, Chromosome 5. **c**, Chromosome 9. The allorecognition and framework genes are indicated for each haplotype.

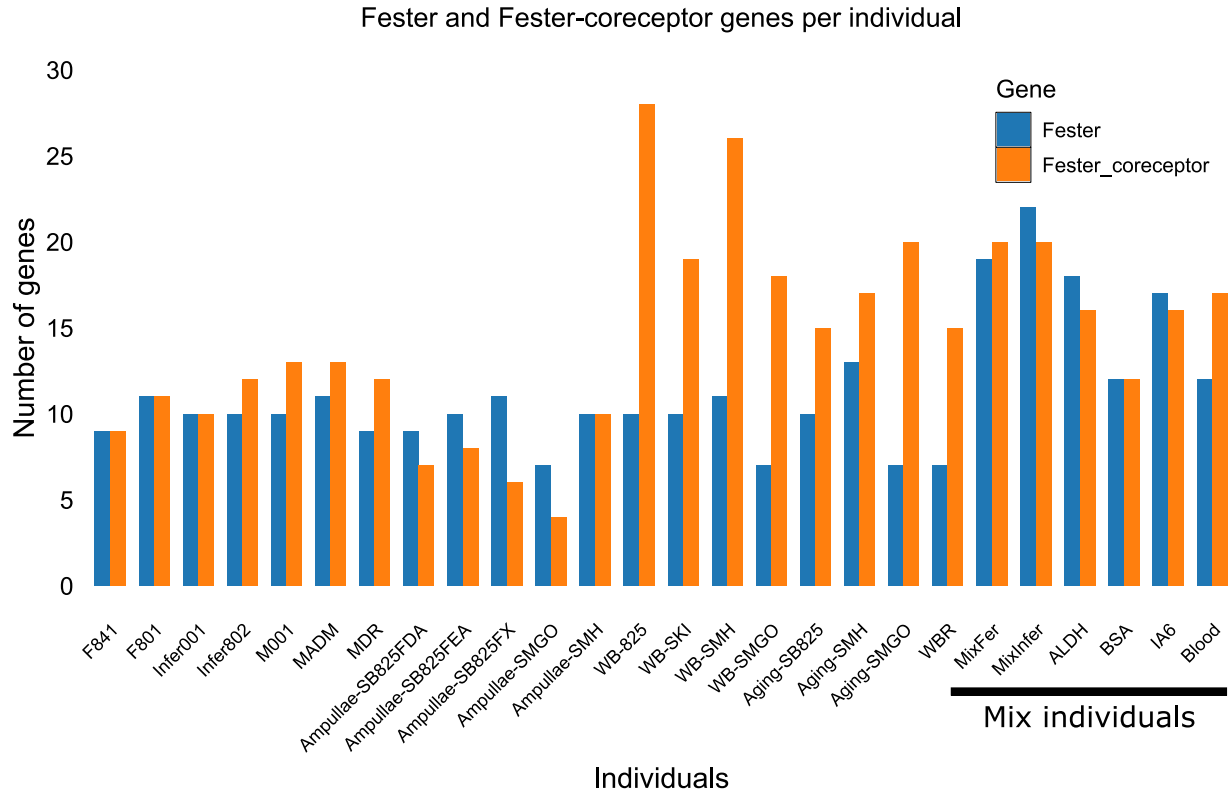
Extended Data



Extended Data Fig. 1 Allorecognition in *Botryllus schlosseri* a, When two colonies grow close together, the ampullae reach out and interact (white arrows), and this will result in one of two outcomes: either the two ampullae will fuse **b**, allowing the circulation of the two colonies to interconnect (white arrows), or they will reject each other (**c,d**). Rejection is a localized inflammatory reaction where blood cells leak from the ampullae. **c**, A close-up of rejecting ampullae showing cell leakage. Once outside the circulation, cells discharge their vacuoles, initiating a prophenoloxidase pathway which eventually forms dark melanin scars, called points of rejection, or POR (**c**, black arrow on right; **d** white arrows). The ampullae then disintegrate (left of POR, top white arrow in **d**), and the colonies no longer interact. The reaction takes ~24-48h to occur and is controlled by a single highly polymorphic locus called the *fuhc* (for fusion/histocompatibility). Colonies will fuse if they share one or both alleles, and will reject if no alleles are shared. **e**, Lower magnification shows a single individual, consisting of multiple zooids occupying the center. The large extracorporeal vasculature and terminating ampullae are outlined (large arrows). In this experiment, a colony was placed between a compatible partner (bottom) and an incompatible partner (top). As shown, a colony can simultaneously fuse (red arrows) and reject (small black arrows, top). This demonstrates that allorecognition is spatially segregated and occur independently at the tips of the ampullae that are in contact.

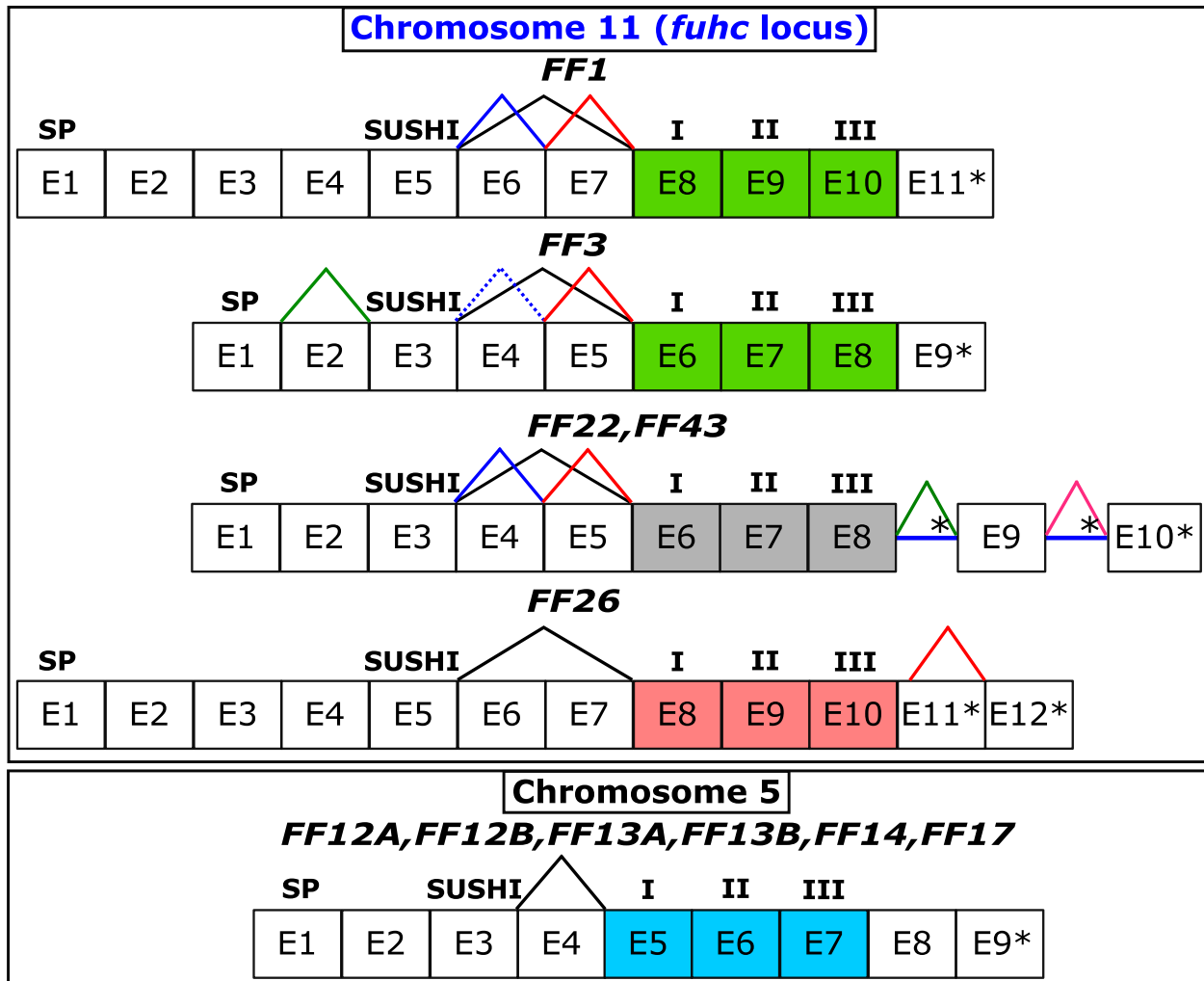


Extended Data Fig. 2 Identity matrix for fester and FcoR genes. **a**, Identity matrix of *fester* genes. **b**, Comparison of identity between the *fester* genes and FF1 alleles. **c**, Identity matrix of *FcoR* genes. **d**, Comparison of identity between the *FcoR* genes and *FcoR7* alleles. We used the range of amino acid and nucleotide identify from FF1 and *FcoR7* alleles as a benchmark to predict alleles vs. loci of the new sequences. If sequences shared >82% amino acid homology and >90% nucleotide homology over the entire gene, they were classified as alleles.

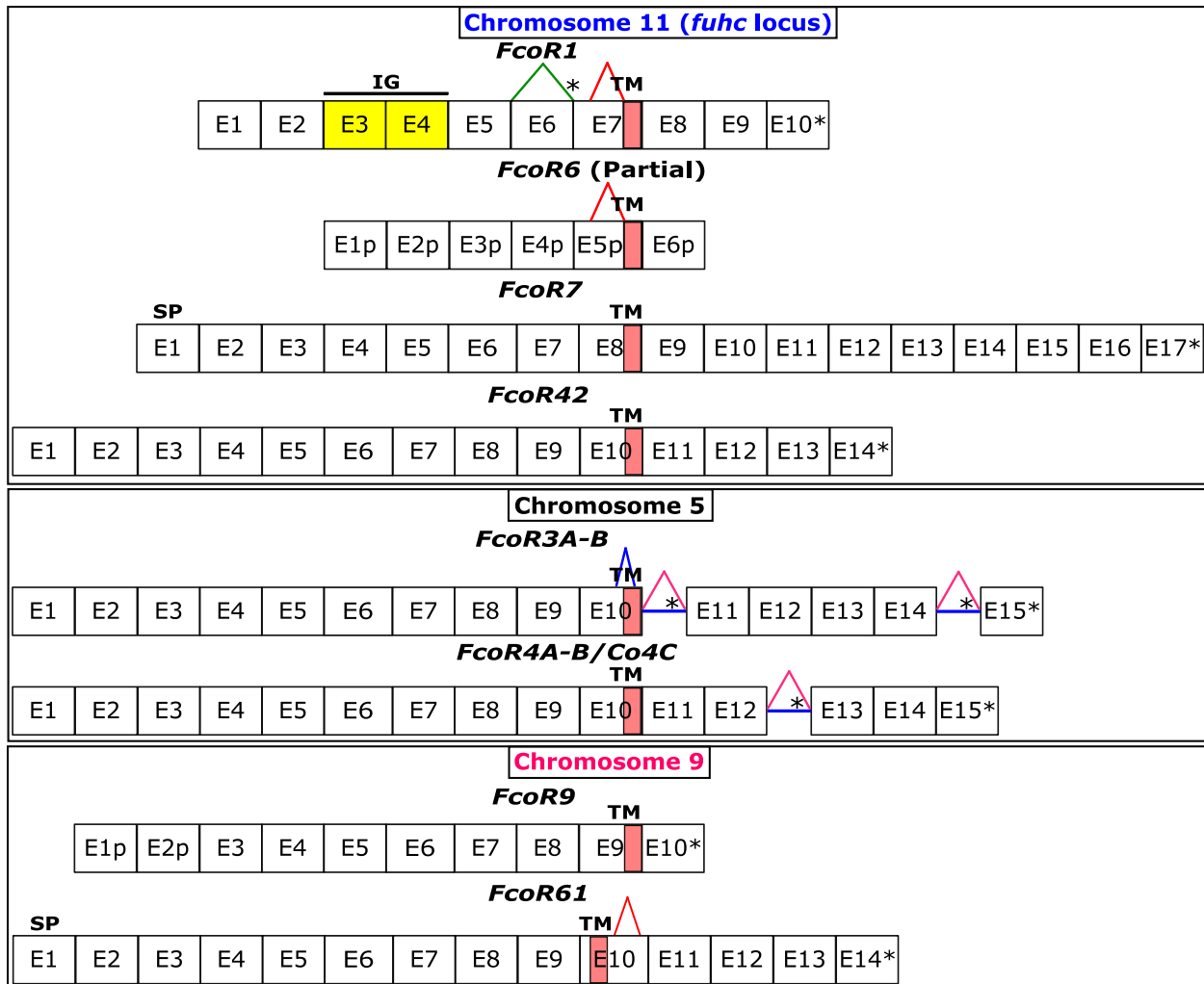


Extended Data Fig. 3 Expression of *fester* and *FcoR* genes. *fester* and *FcoR* genes were quantified in different individuals of *B. schlosseri* using transcriptome assemblies. The last six samples on right contain a mix of individuals.

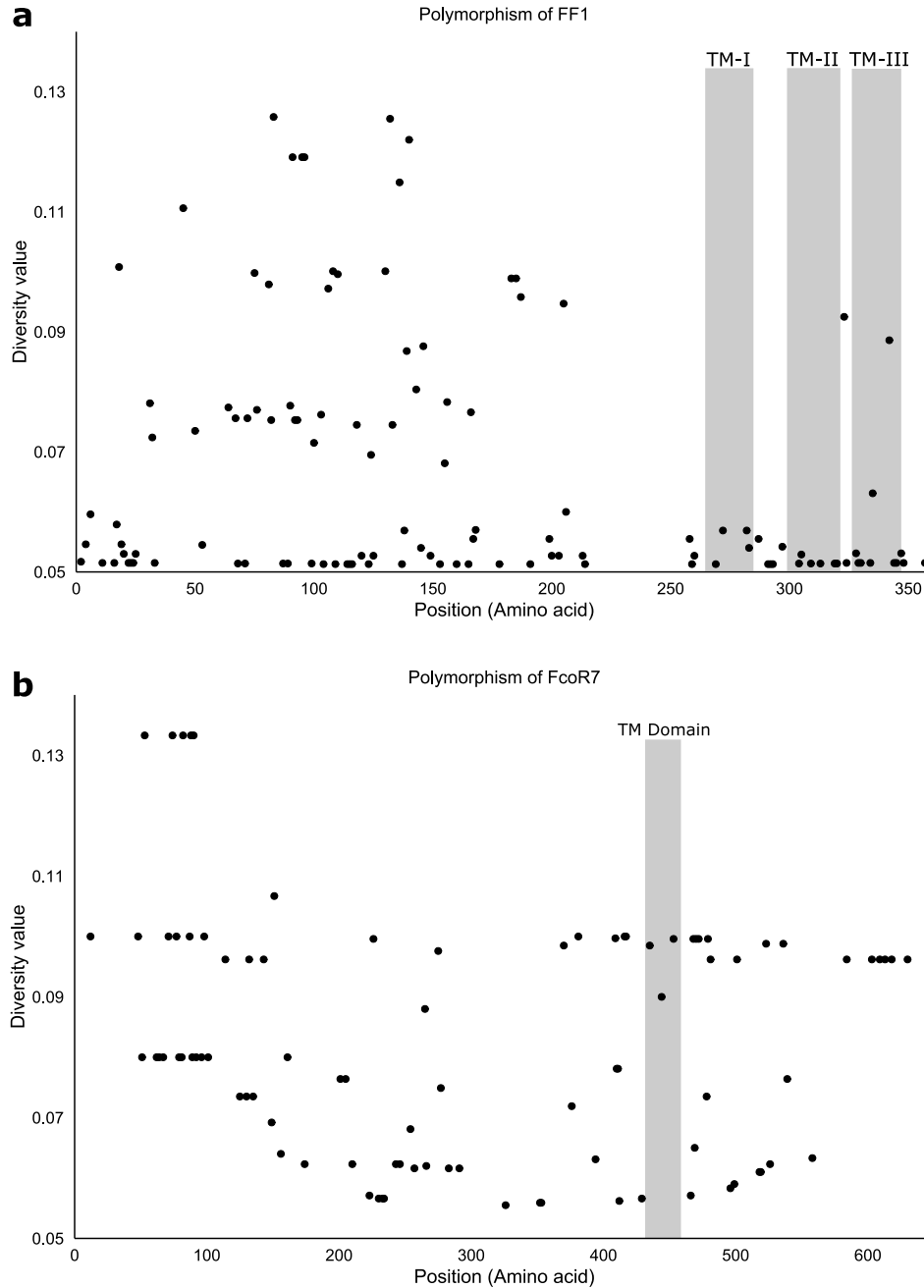
a



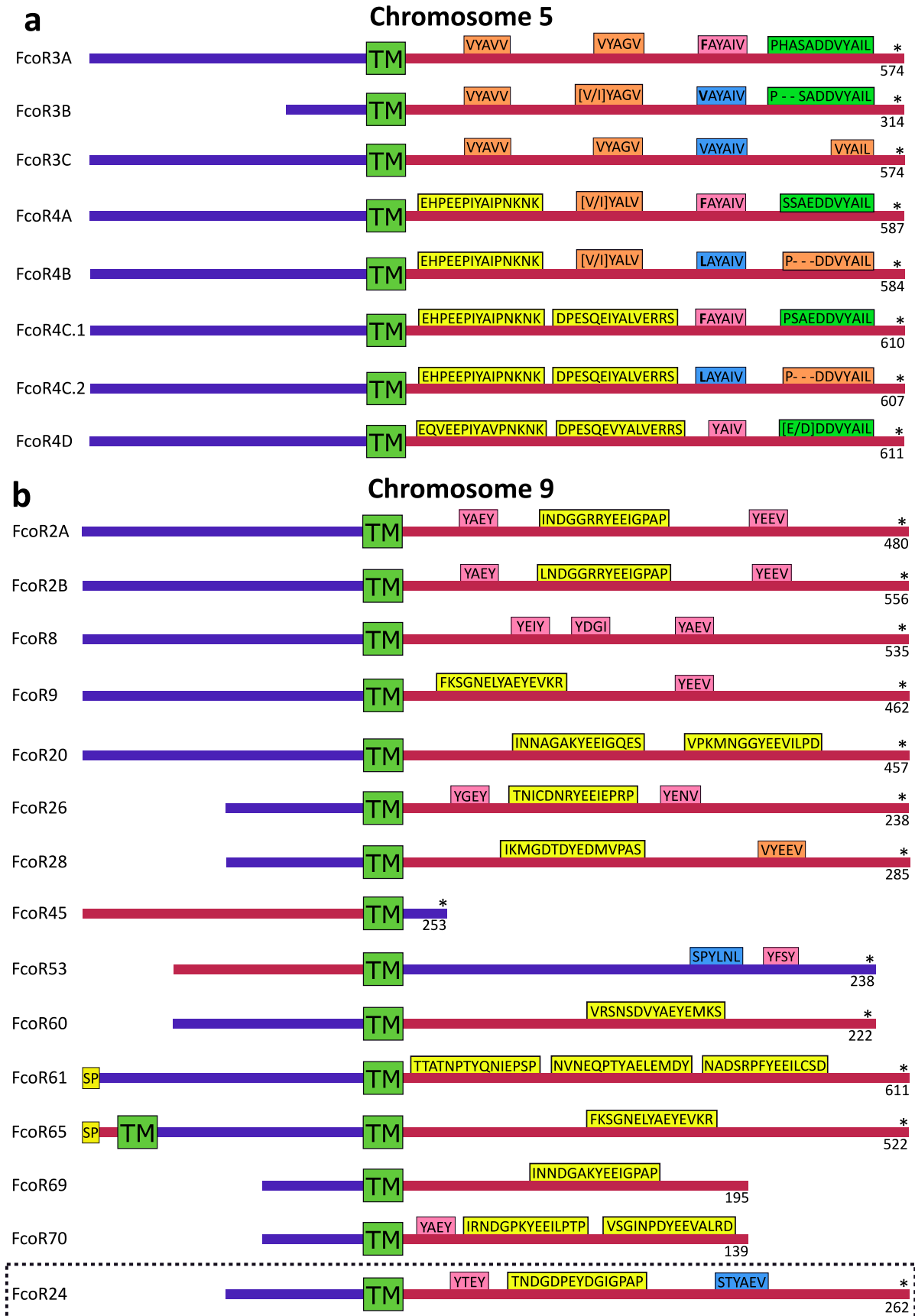
b

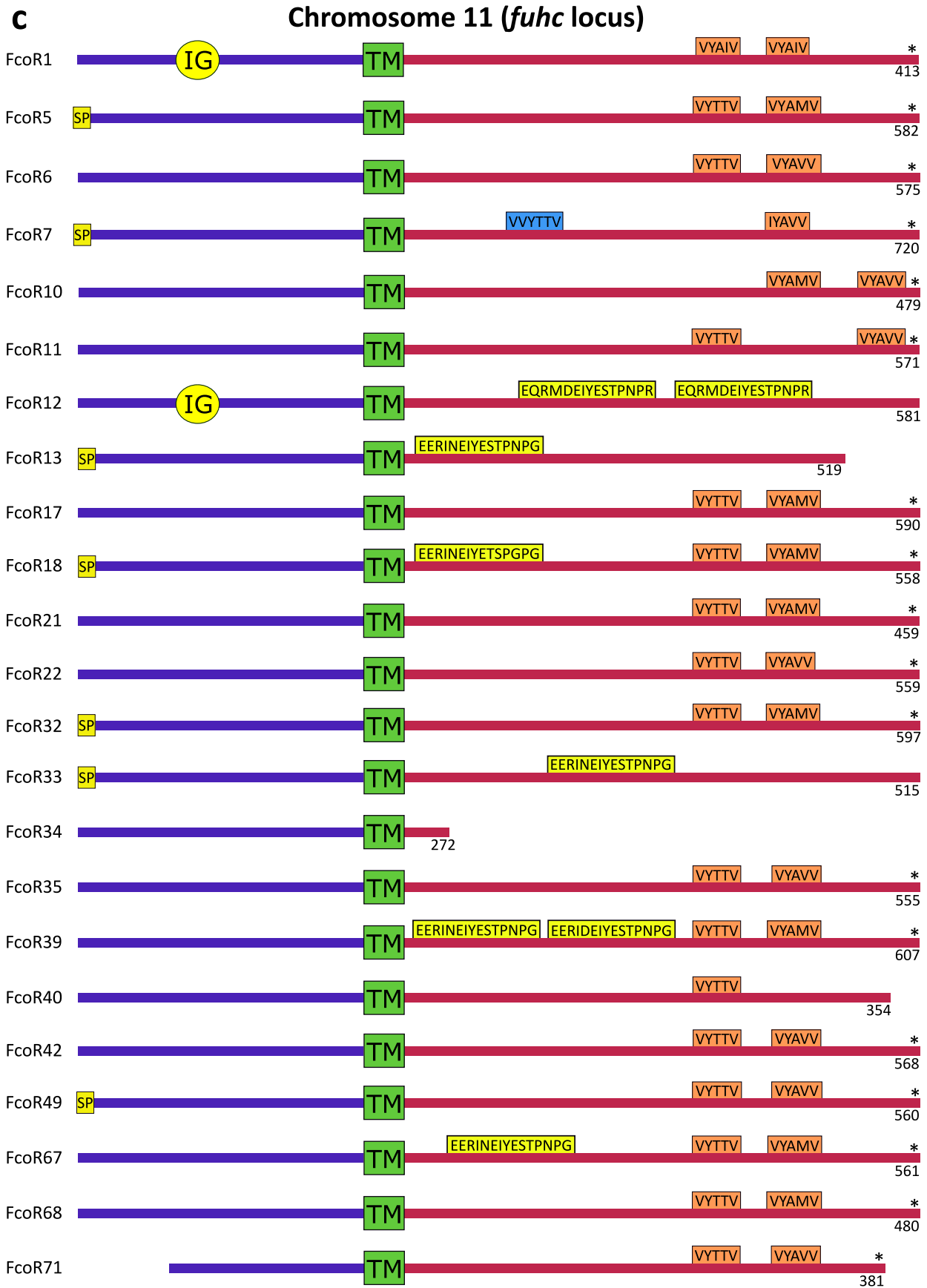


Extended Data Fig. 4 Genomic structure and alternative splicing of *fester* and *FcoR* genes. **a**, *Fester* genes exhibit two regions with alternative splicing. The first region is between the Sushi domain and the first transmembrane domain. The second region is located in the cytoplasmic region. Exons encoding the transmembrane domains are highlighted in colors. **b**, *FcoR* genes exhibit alternative splicing in the extracellular and intracellular regions. Asterisks represent stop codons. Intron retentions are indicated with blue horizontal lines. Signal peptide: SP. I, II, and III: First, second and third transmembrane domains, respectively.



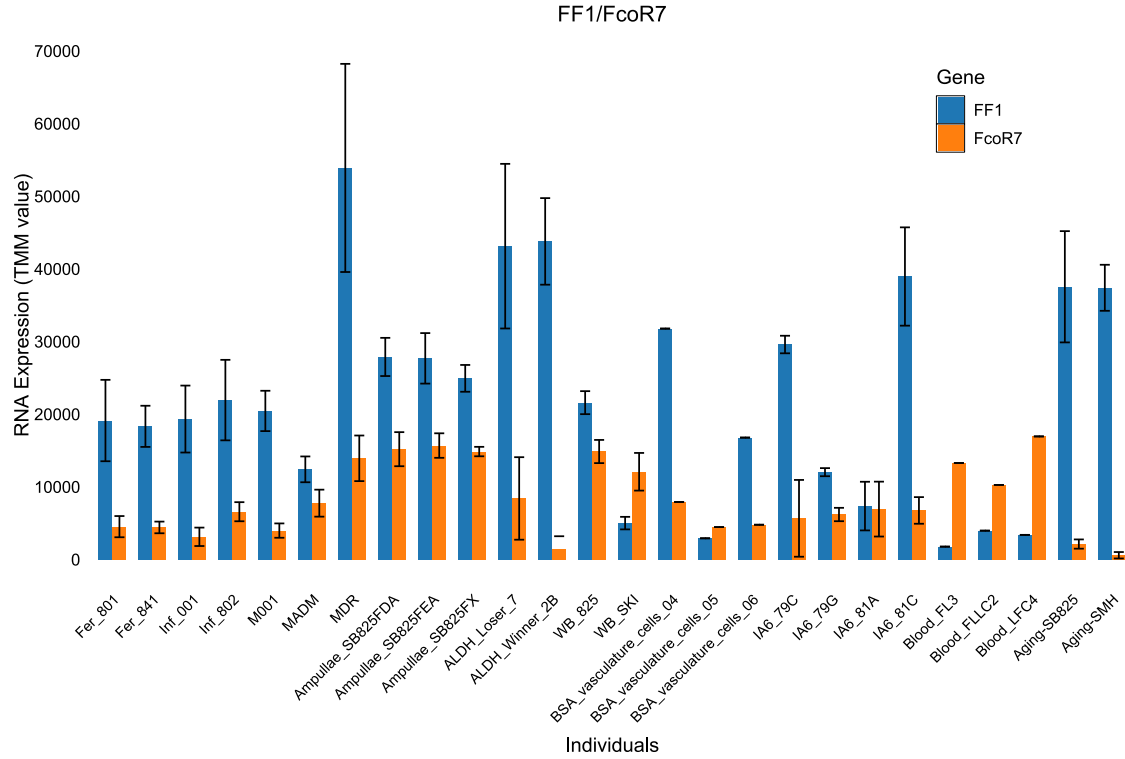
Extended Data Fig. 5 Distribution of polymorphic residues in FF1 and FcoR7 alleles. **a**, 77 allotypes of the FF1 protein and, **b**, Twenty allotypes of the FcoR7 protein were compared using DIVAA. Only variable residues are represented. Amino acid position and diversity value are represented in the X-axis and Y-axis, respectively. A diversity value of 1 for a particular position means that any amino acid is as likely as any other to be present at that position. A diversity value of 0.05 is consistent with 100% conservation at that site (1/20 possible amino acids). TM: Transmembrane domain.



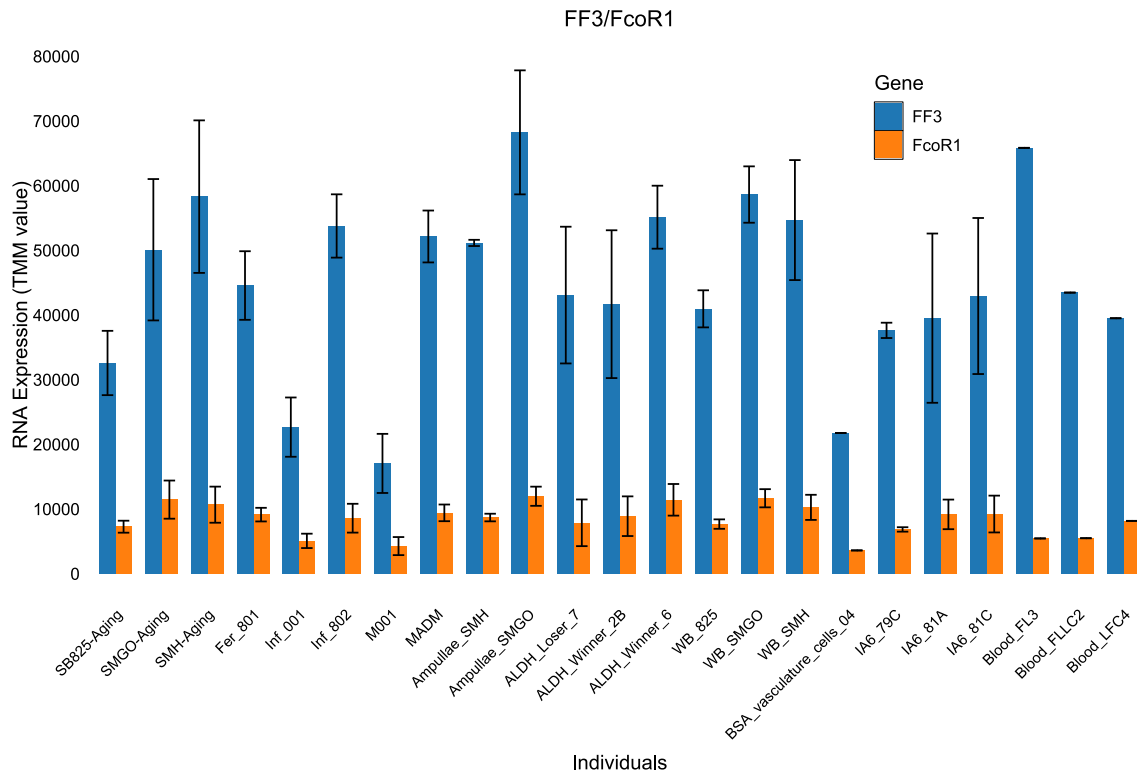


Extended Data Fig. 6 Structure of FcoR proteins. Protein structure of FcoR proteins located on: **a**, chromosome 5. **b**, chromosome 9. **c**, chromosome 11. SP: Signal peptide. IG: Immunoglobulin domain. TM: Transmembrane domain. ITIM, hemITAM, SH2, Tyrosine core-1 (YxxY/L/V/I) and Tyrosine core-2 (V/IYxxV/L) motifs are highlighted in blue, green, yellow, pink and orange colors, respectively. Blue and red lines represent the extracellular and intracellular regions of FcoR proteins, * = stop codon. FcoR proteins without a SP are not likely full-length, as there is no initiator methionine. Partial sequences without a transmembrane domain are not shown.

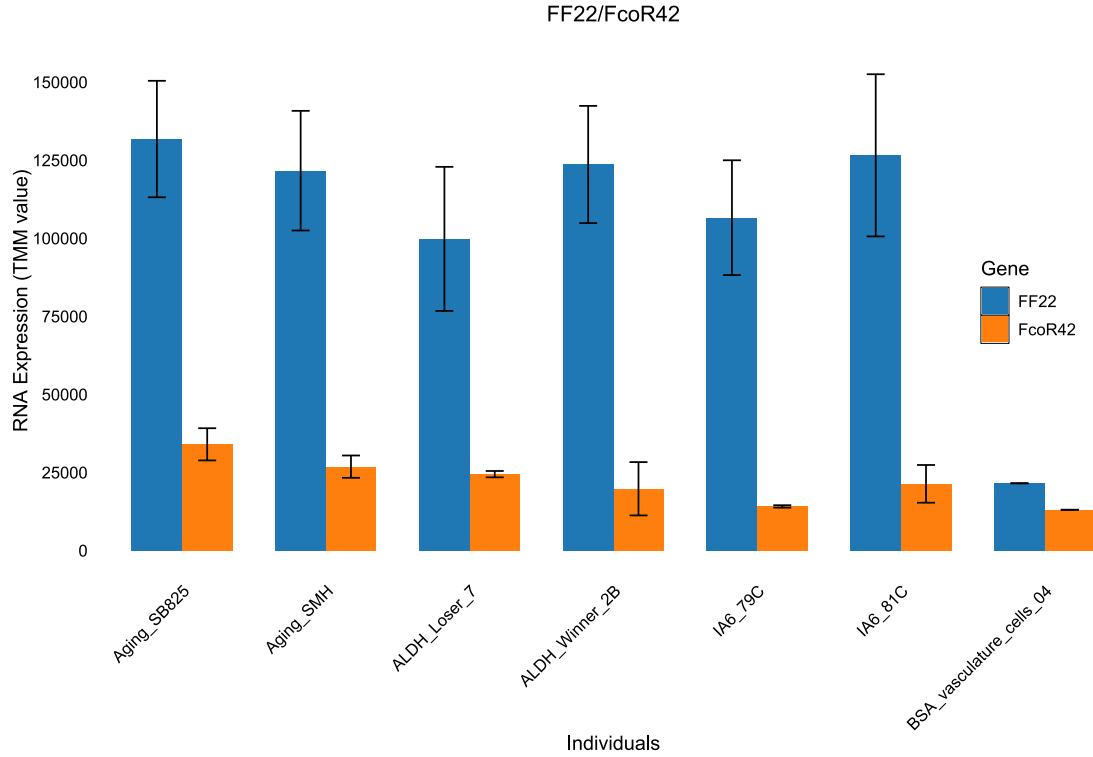
a



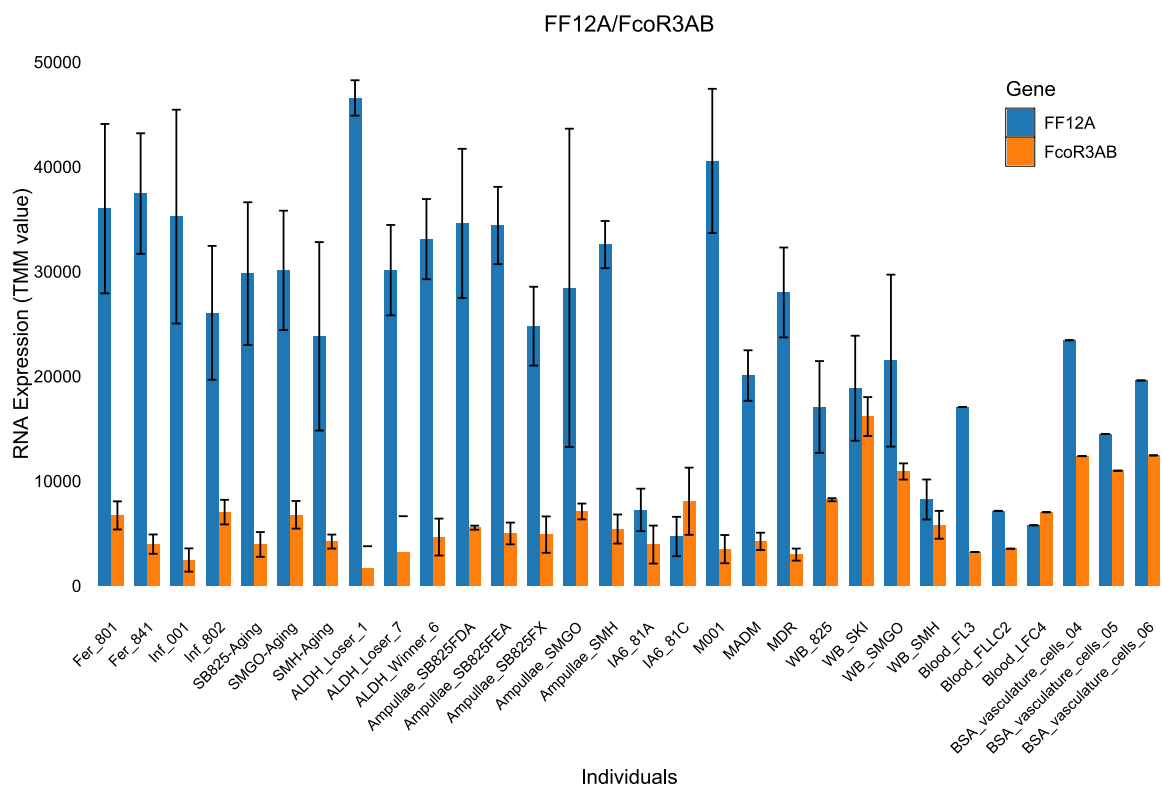
b



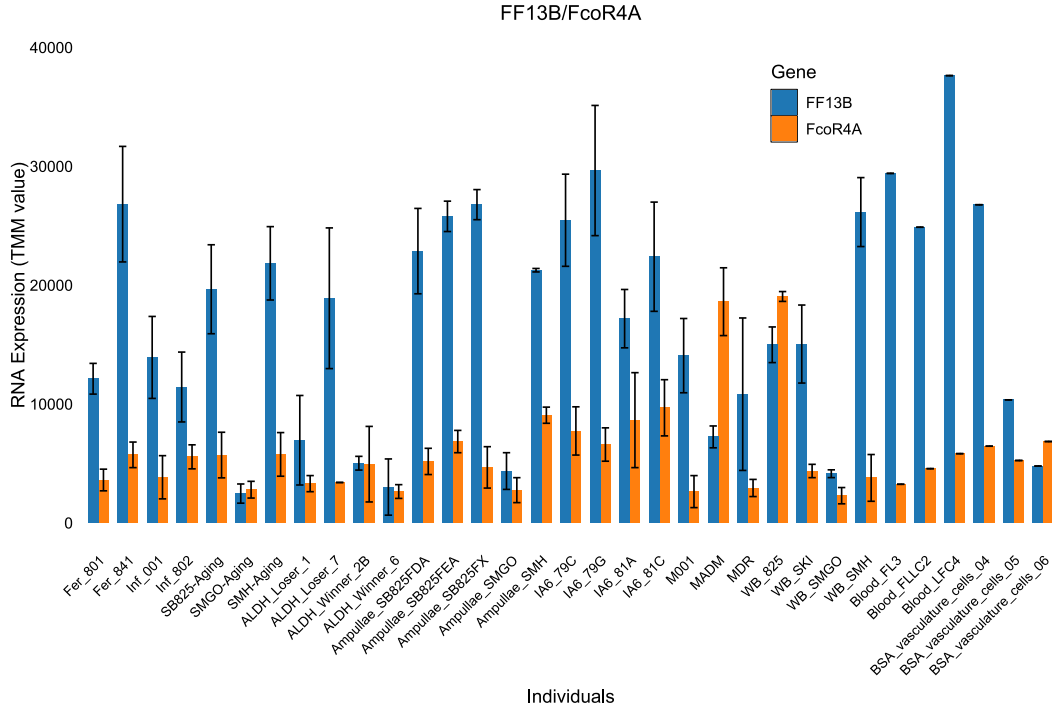
c



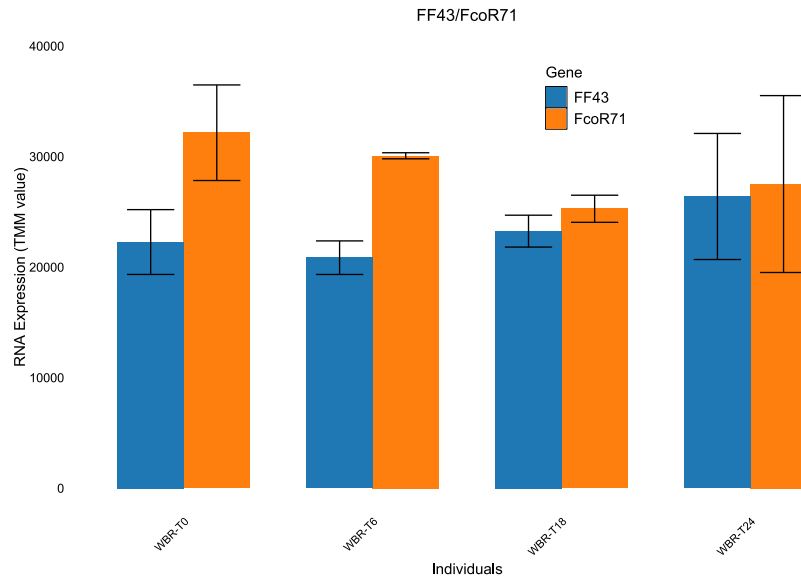
d



e

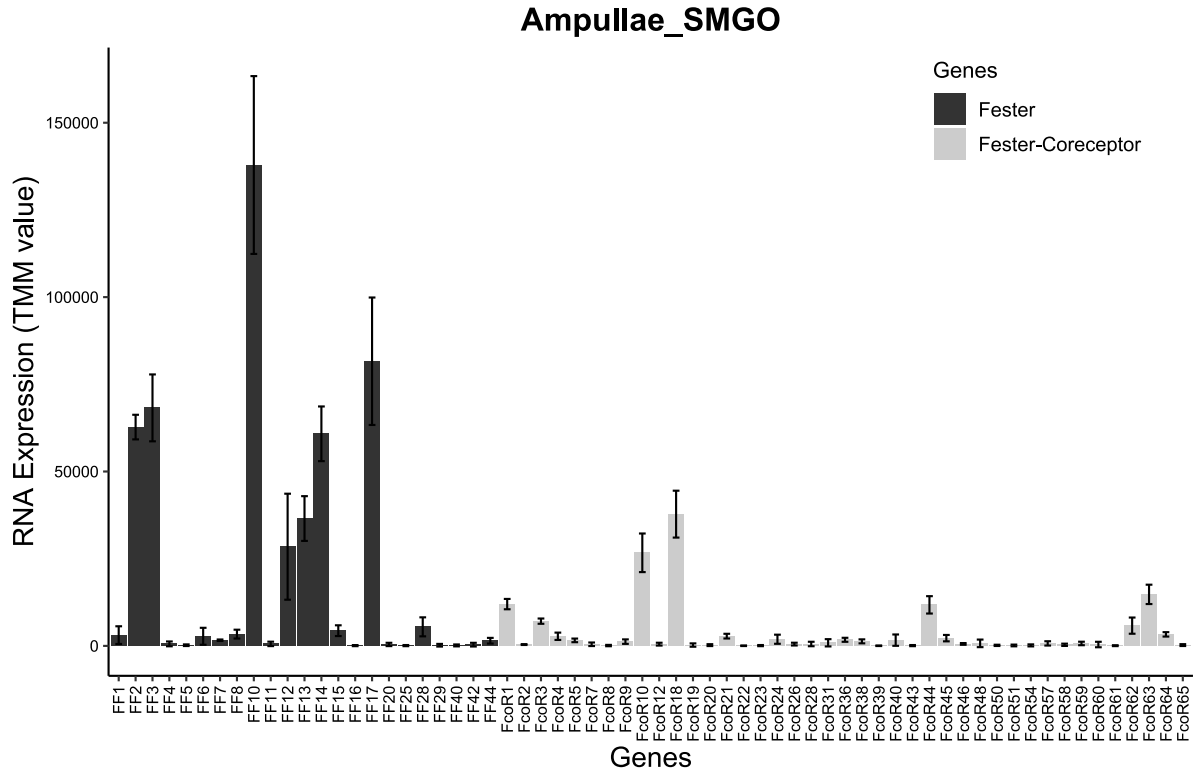


f

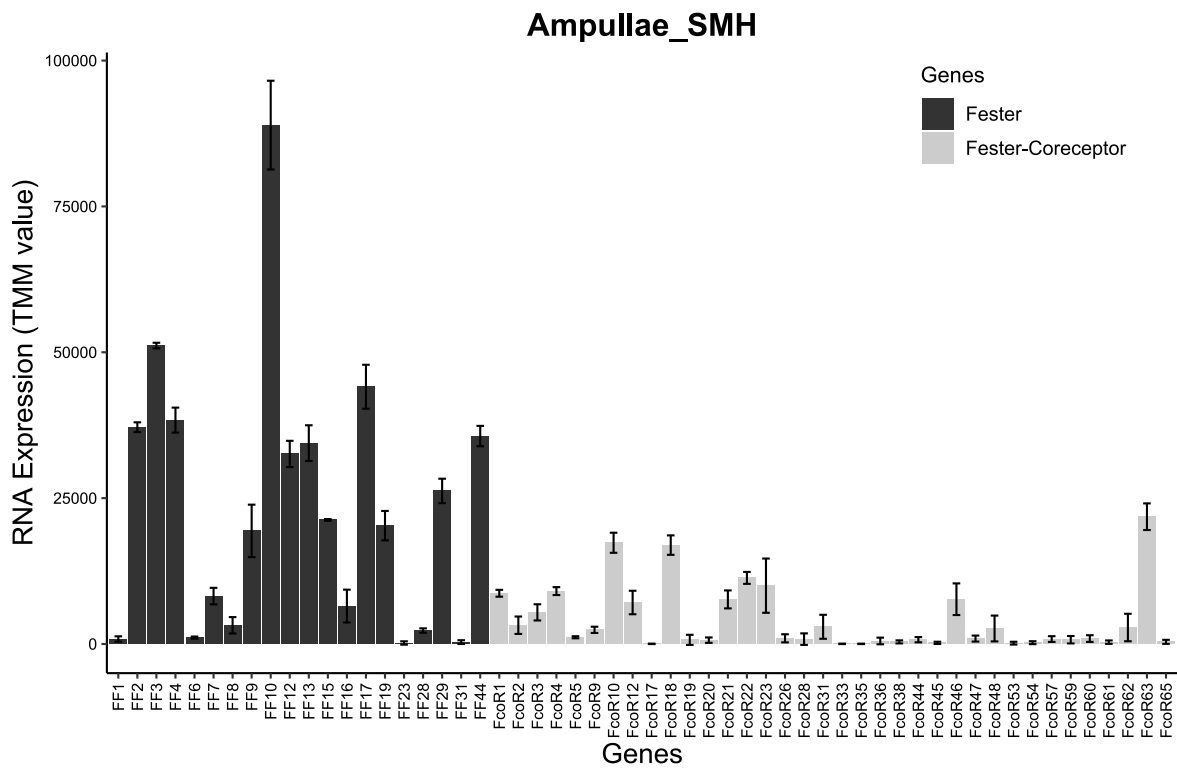


Extended Data Fig. 7 Co-expression of *fester* and *FcoR*. *fester* and *FcoR* gene pairs were quantified in different individuals of *B. schlosseri*. X-axis shows different *Botryllus* individuals, and Y-axis shows gene expression levels (TMM units).

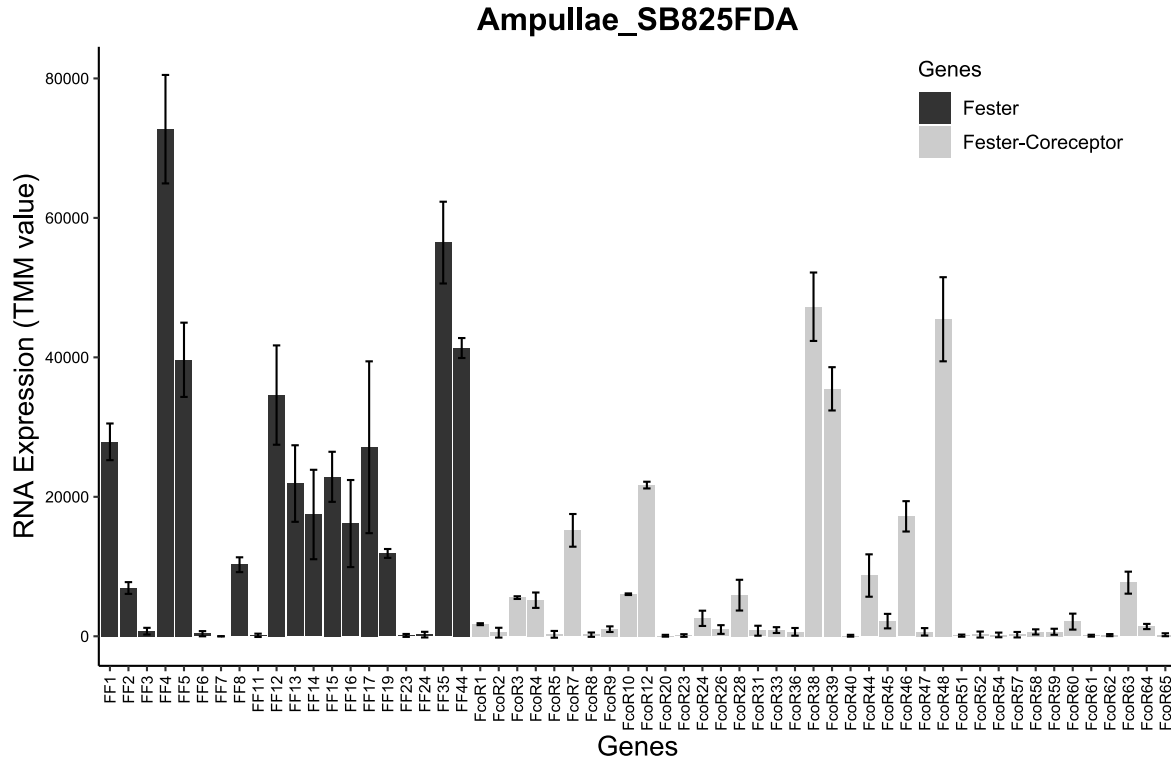
a



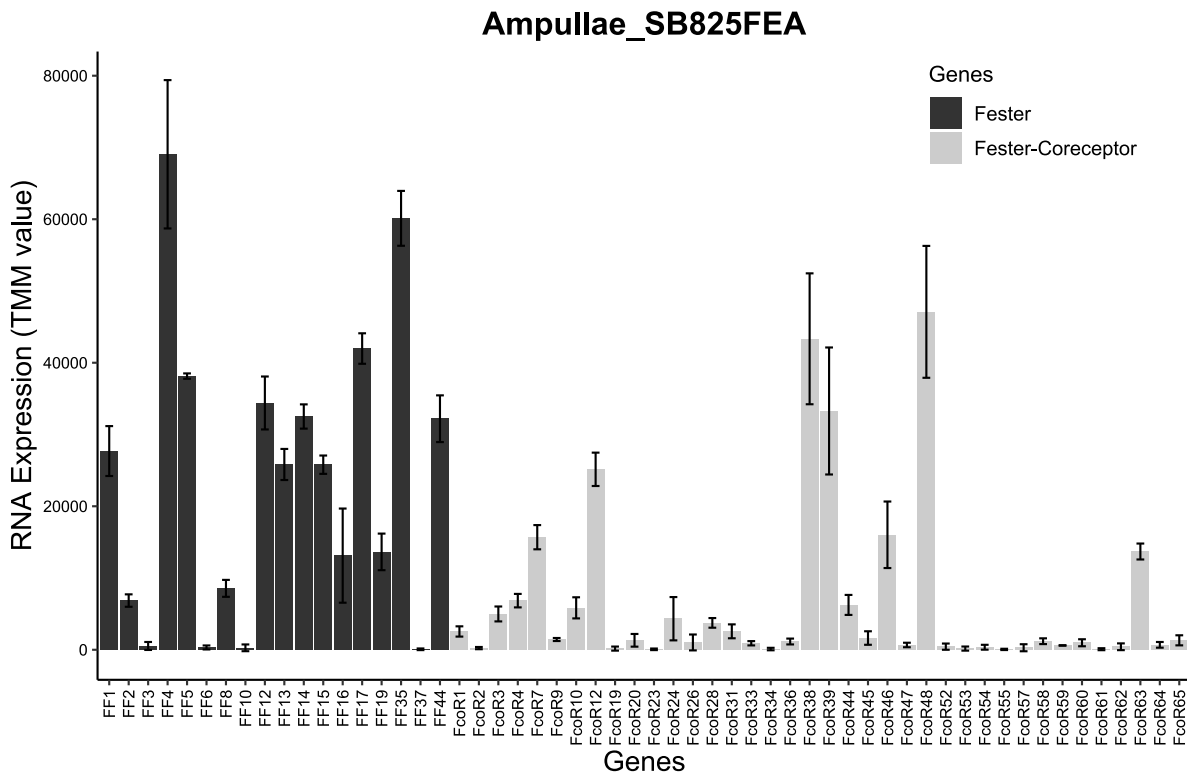
b



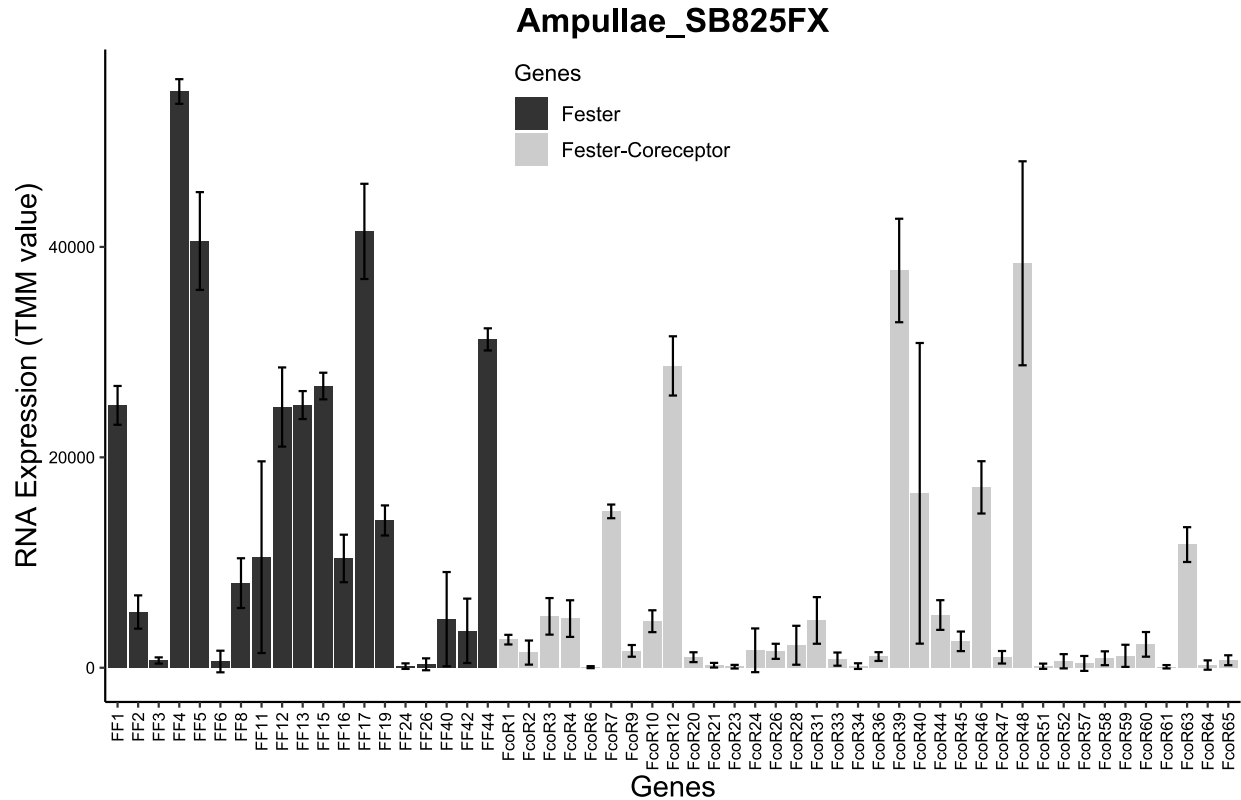
c



d

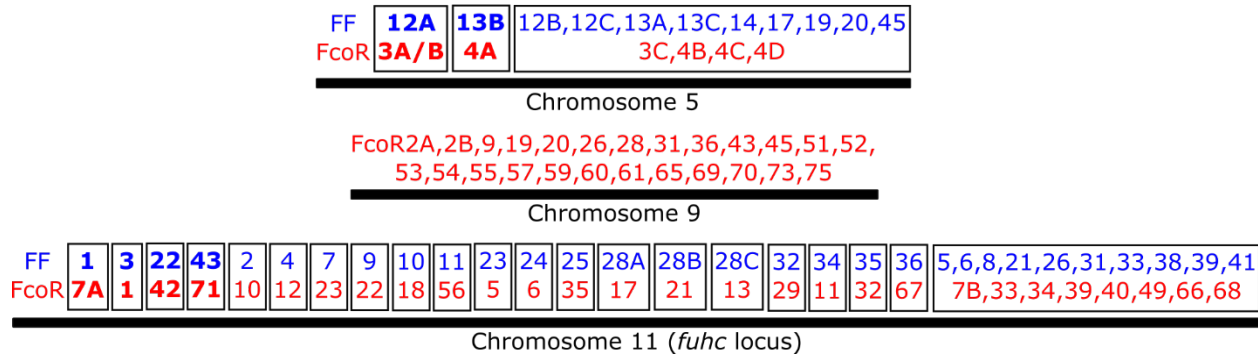


e



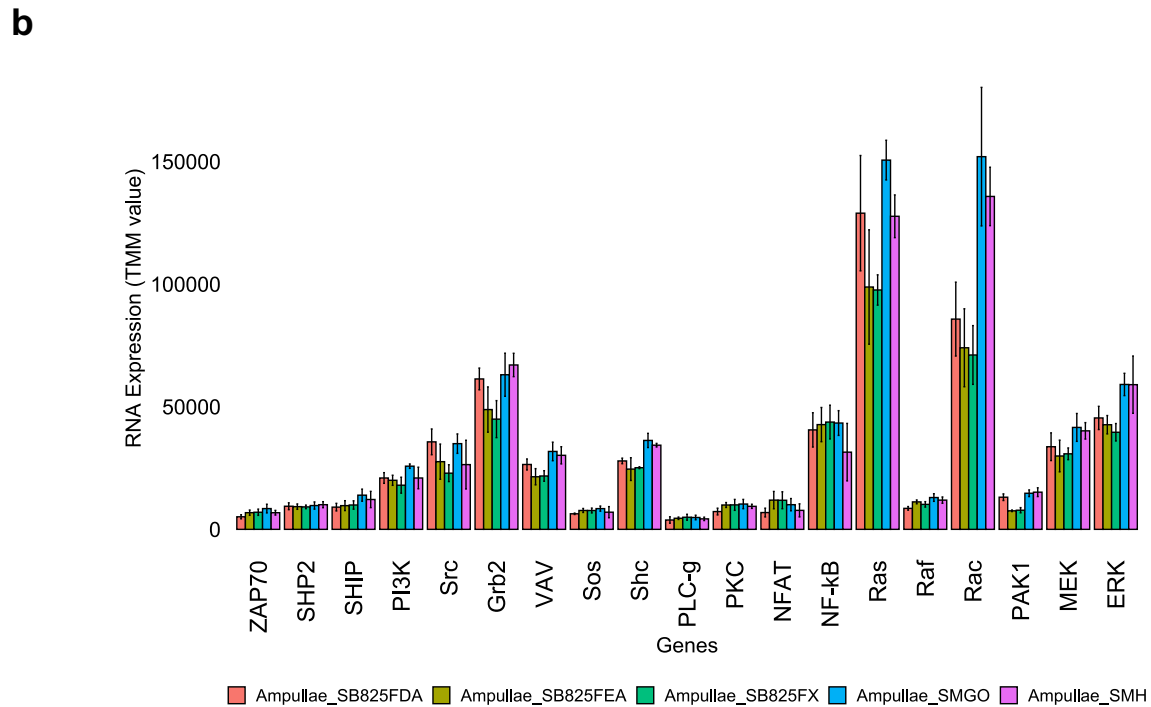
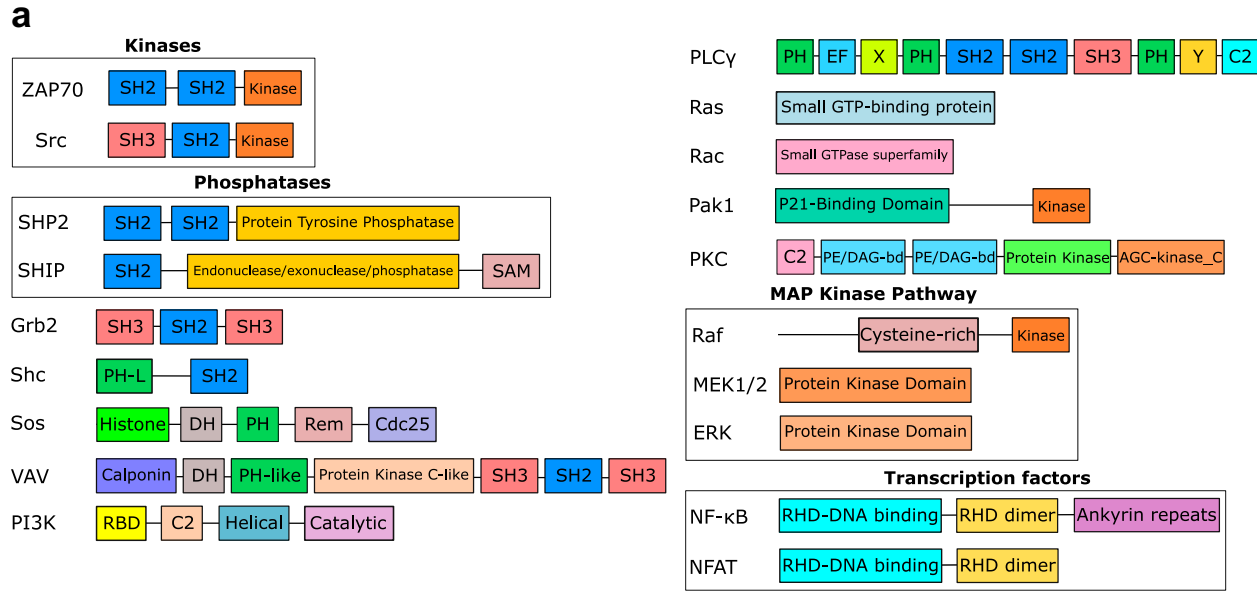
Extended Data Fig. 8 Unique repertoire and stable expression of *fester* and *FcoR* genes in ampullae isolated from 5 individuals (a-e). In each individual, ampullae were surgically removed and collected, the vessels regenerated, and this tissue isolation/regeneration was done three times. mRNA isolated from each sample was sequenced, and the average expression (Y axis, TMM units) of each FF and FcoR gene (X-axis) levels are shown. Each individual expresses a unique repertoire of FF and FcoR genes, and expression levels are stable following multiple cycles of ablation/regeneration.

Putative genomic localization of *fester* (FF) and *fester-coreceptor* (FcoR) genes



Extended Data Fig. 9 Predicted genomic localization of *fester* and *FcoR* genes.

Predicted genomic localizations were estimated based on phylogenetic similarity between genes and chromosomal regions. Gene pairs were established using both phylogenetic, genomic and transcriptomic data. *fester* and *FcoR* genes are highlighted in blue and red, respectively. The genomic localizations of the genes highlighted in bold have been confirmed.



Extended Data Fig. 10 Structure and expression of proteins involved in ITAM and ITIM signaling from *B. schlosseri*. **a**, domain architecture of homologs of the indicated genes were identified in the transcriptome of *B. schlosseri*. **b**, expression of these genes was quantified in the vasculature system of five *B. schlosseri* individuals. Genes are plotted in the x-axis and RNA expression (TMM units) is plotted in the y-axis. Means and standard deviations were calculated between three or four replicates per individual.

Extended Data Table 1. Transcriptomes of *B. schlosseri* analyzed in this study

Transcriptomes	Individuals	Accession number
Fertility-Blastogenesis	Fertile841, Fertile801, Infer001, Infer802, Mix Fertile, Mix Infertile	PRJNA263209
Aging	SB825, SMH, SMGO	PRJNA474433
Whole Body	SB825, SMH, SMGO, SKI	De Tomaso Lab (Jon Schultz). This study
Male	MDR, M001, MADM	De Tomaso Lab (Delany Rodriguez). This study
Vasculature (Ampullae)	SB825-FDA, SB825-FEA, SB825-FX, SMGO, SMH	De Tomaso Lab (Daryl Taketa). This study
ALDH Winner Loser	Loser 1, Loser 7, Winner 2B, Winner 6	De Tomaso Lab. This study
BSA Vascular Cells (Ampullae)	Not specified	PMC3988187
Blood	FL3, FLLC2, LFC4	De Tomaso Lab (Shambhavi Singh). This study
IA6 Winner Loser	81A, 81C	De Tomaso Lab. This study
Whole-body regeneration (WBR)	Isogenic strain	PRJNA798022

Extended Data Table 2. Primers used in this study for *B. schlosseri*

Genes	Primers (5' to 3')	Product size (bp)
<i>FF1-genomic</i>	Fwd: CCAAGGCGCTAGGAAAGACT Rev: CCTCGACTTTCAAAGTATTTGTCT	143
<i>FF2-genomic</i>	Fwd: TGTGAGTGATCTGGAAAATCTTACA Rev: GTGAAACATTCAAAGAAAGCTTCTT	134
<i>FF3-genomic</i>	Fwd: GATGGCTGCACCAACTACTACTC Rev: TCTTTGTAGAAACTGATTATTCAATCC	141
<i>FF4-genomic</i>	Fwd: ATCAATGCTCTTAAGTCCAACAA Rev: CTTTAACAGCAAGTTTGTGAATCAA	145
<i>FF5-genomic</i>	Fwd: CTCAAACGTAACAAGACTACATTG Rev: ATAAGTCCAATTTGATGTTGAC	147
<i>FF7-genomic</i>	Fwd: GCAGTGCTACAGCAAATTGTTC Rev: AGCTGTACTGGTGTGCCTAAAGT	142
<i>FF9-genomic</i>	Fwd: TTCAAGCACTACATTCACCATAA Rev: CTGTTGCACTGGTACATCTAGGG	241
<i>FF12-genomic</i>	Fwd: TTGATGCTCAAAGCAAGCAAG Rev: AGTCGCATCCATTATAGCCATC	215
<i>FF13-genomic</i>	Fwd: TCTGCGAAGTTGGTGATGATTTTA Rev: AAGTGGTACCATGTCATCAGG	167
<i>FF16-genomic</i>	Fwd: AAGTTTCTCCTTTCATACTATTACCG Rev: TAATTCCAGATGAGACTGTGTGC	240
<i>FF17-genomic</i>	Fwd: TTGGACACCGACTTCGCATA Rev: CGTAAACGTTCCGAATATTCATGTC	241

<i>FF22-genomic</i>	Fwd: CACTTTGTGTAAGGTCTCTCAACA Rev: CTGCAAGATGGTCACAGGAGAT	359
<i>FF1-mRNA</i>	Fwd: CCAATTGTAGTTGAAGAGTAACAATG	1206
<i>FF2-mRNA</i>	Fwd: GTACCGTACTGCTTCATATGAATG	1222
<i>FF3-mRNA</i>	Fwd: ATGGGATTGGAATTATTTATGATG	1168
<i>FF4-mRNA</i>	Fwd: GTAACCAACATGAAAGGATCAATG	1186
<i>FF5-mRNA</i>	Fwd: AGATTATTTTCATTGCATTCTGGAC	1189
<i>FF7-mRNA</i>	Fwd: TTAAGCAGATTTCTATAGTTAATCAAATG	1257
<i>FF1,2,3,4,5,7</i>	Rev: GACAAGACGTGGTAAAATACATTAAG	N/A
<i>FF12-mRNA</i>	Fwd: GTTTCAGCAGGACAACCATCA Rev: ACAGTTTTACTTCTTTTCCAGGTATC	1101
<i>FF13-mRNA</i>	Fwd: TTGTGATGTCAAACCTGCATCC Rev: TGAGAMTACCRACTATTGTTCCAG	939
<i>FF16-mRNA</i>	Fwd: AATTGGCACTTTTCATCTCCTT Rev: CTACAGTTTTACTTCTTTTCCAGGTAT	1058
<i>FF17-mRNA</i>	Fwd: TTTCTTGAACCTGCGTCCATTC Rev: GTTTGACATCTTTTCCAGGTATCC	1028
<i>FF22-mRNA</i>	Fwd: TGTTGTTAGCAGCTCTTGTTCA Rev: ACACATTGAGATGACAACAGAAGAA	1181

Extended Data Table 3 is a converted Excel file over the next 18 pages

			PAIR-1		PAIR-2	
			FESTER	COREC	FESTER	COREC
Number of transcriptome	Transcriptomes	Individual/Group of individuals	FF1	Co7	F12A/B/	Co3A/B/C
1	F841	Ind1	Yes	Yes	Yes	Yes
2	F801	Ind2	Yes	Yes	Yes	Yes
3	Infer001	Ind3	Yes	Yes	Yes	No
4	Infer802	Ind4	Yes	Yes	Yes	Yes
5	M001	Ind5	Yes	Yes	Yes	Yes
6	MADM	Ind6	Yes	Yes	Yes	Yes
7	MDR	Ind7	Yes	Yes	Yes	Yes
8	Ampullae_SB825FDA	Ind8	Yes	Yes	Yes	No
9	Ampullae_SB825FEA	Ind9	Yes	Yes	Yes	No
10	Ampullae_SB825FX	Ind10	Yes	Yes	Yes	No
11	Ampullae_SMGO	Ind11	No	No	Yes	No
12	Ampullae_SMH	Ind12	No	No	Yes	Yes
13	WB_825	Ind13	No	Yes	Yes	Yes
14	WB_SKI	Ind14	Yes	Yes	Yes	Yes
15	WB_SMH	Ind15	No	No	Yes	Yes
16	WB_SMGO	Ind16	No	No	Yes	Yes
17	Aging-SB825	Ind17	Yes	Yes	Yes	Yes
18	Aging-SMH	Ind18	Yes	No	Yes	Yes
19	Aging-SMGO	Ind19	No	No	Yes	Yes
20	WBR (Ricci, et al. 2022)	Ind20	Yes	Yes	Yes	Yes
21	MixF	Grp1	Yes	Yes	Yes	Yes
22	MixInfer	Grp2	Yes	Yes	Yes	Yes
23	ALDH	Grp3	Yes	Yes	Yes	Yes
24	BSA_vasculature	Grp4	Yes	Yes	Yes	Yes
25	IA6-Mix	Grp5	Yes	Yes	Yes	Yes
26	Blood-Mix	Grp6	Yes	Yes	Yes	Yes
	Frequency		20	20	26	21
	ITIM		N/A	Yes	N/A	Yes*

Tyrosine-motifs	hemITAM		N/A	No	N/A	Yes*
	SH2		N/A	No	N/A	No
	Tyrosine core-1 (YxxY/L/V/I)		N/A	No	N/A	No
	tyrosine core-2 ([E/D][V/I]YxxV/L)		N/A	Yes	N/A	Yes
	Presence of TM and cytoplasmic region with a stop codon?		N/A	Present	N/A	Present

PAIR-3		PAIR-4		PAIR-5		PAIR-6		PAIR-7		PAIR-8		PAIR-9
FESTER	COREC	FESTER	COREC	FESTER	COREC	FESTER	COREC	FESTER	COREC	FESTER	COREC	FESTER
13A/B/C	Co4	FF3	Co1	FF4	Co12	FF7	Co23	FF10	Co18	FF2	Co10	FF9
Yes	Yes	No	Yes	Yes	Yes	No	No	No	No	Yes	Yes	No
Yes	Yes	Yes	Yes	No	No	Yes	No	Yes	Yes	Yes	Yes	No
Yes	Yes	Yes	Yes	No	No	Yes	Yes	Yes	Yes	Yes	Yes	Yes
Yes	Yes	Yes	Yes	No	No	No	No	Yes	Yes	Yes	Yes	No
Yes	Yes	Yes	Yes	No	No	Yes	Yes	Yes	Yes	Yes	Yes	Yes
Yes	Yes	Yes	Yes	Yes	Yes	Yes	Yes	No	No	No	No	No
Yes	Yes	No	No	Yes	Yes	Yes	Yes	No	No	No	No	No
Yes	Yes	No	Yes	Yes	Yes	No	No	No	No	No	No	No
Yes	Yes	No	Yes	Yes	Yes	No	No	No	No	No	Yes	No
Yes	Yes	No	No	Yes	Yes	No	No	No	No	No	No	No
Yes	Yes	Yes	Yes	No	No	No	No	Yes	Yes	Yes	Yes	No
Yes	Yes	Yes	Yes	Yes	Yes	No	Yes	Yes	Yes	Yes	Yes	Yes
Yes	Yes	Yes	Yes	No	No	Yes	Yes	No	No	No	No	No
Yes	Yes	No	No	Yes	Yes	No	No	No	No	No	No	No
Yes	Yes	Yes	Yes	Yes	Yes	Yes	Yes	Yes	Yes	Yes	Yes	Yes
Yes	Yes	Yes	Yes	Yes	Yes	No	No	Yes	Yes	Yes	Yes	No
Yes	Yes	Yes	Yes	No	No	No	No	Yes	Yes	Yes	Yes	No
Yes	Yes	Yes	Yes	Yes	Yes	No	No	No	No	No	No	Yes
Yes	Yes	Yes	Yes	Yes	No	Yes	Yes	Yes	Yes	Yes	Yes	Yes
Yes	Yes	Yes	Yes	No	No	No	No	Yes	Yes	Yes	Yes	No
Yes	Yes	No	No	No	No	No	No	No	No	No	No	No
Yes	Yes	Yes	Yes	Yes	Yes	Yes	Yes	Yes	Yes	Yes	Yes	Yes
Yes	Yes	Yes	Yes	Yes	Yes	Yes	Yes	Yes	Yes	Yes	Yes	Yes
Yes	Yes	Yes	Yes	Yes	Yes	Yes	Yes	No	No	No	No	No
Yes	Yes	Yes	No	Yes	Yes	No	No	No	No	No	No	Yes
Yes	Yes	Yes	Yes	Yes	Yes	Yes	Yes	Yes	No	No	Yes	Yes
Yes	Yes	Yes	Yes	Yes	Yes	No	No	Yes	Yes	Yes	Yes	No
26	26	19	21	17	16	12	12	14	13	14	16	10
N/A	Yes*	N/A	No	N/A	No	N/A	No	N/A	No	N/A	No	N/A

N/A	Yes*	N/A	No	N/A	No	N/A	No	N/A	No	N/A	No	N/A
N/A	Yes	N/A	No	N/A	Yes	N/A	No	N/A	Yes	N/A	No	N/A
N/A	No	N/A	No	N/A	No	N/A	No	N/A	No	N/A	No	N/A
N/A	Yes	N/A	Yes	N/A	No	N/A	No	N/A	Yes	N/A	Yes	N/A
N/A	Present	N/A	Present	N/A	Partial	N/A	Partial	N/A	Present	N/A	Present	N/A

PAIR-16		PAIR-17		PAIR-18		PAIR-19				PAIR-20		PAI
FESTER	COREC	FESTER	COREC	FESTER	COREC	FESTER	COREC	FESTER	COREC	FESTER	COREC	FESTER
FF43	Co71	FF11	Co56	FF24	Co6	FF25	Co35	FF28C	Co13	FF32	Co29*	FF34
No	No	No	No	No	No	No	No	Yes	Yes	No	No	Yes
No	No	No	No	No	No	No	No	No	No	No	No	No
No	No	No	No	No	No	No	No	No	No	No	No	No
No	No	No	No	No	No	No	No	No	No	No	No	No
No	No	No	No	No	No	No	No	No	No	No	No	No
No	No	No	No	No	No	No	No	No	No	No	No	No
No	No	No	No	No	No	Yes	Yes	No	No	No	No	No
No	No	No	No	No	No	No	No	No	No	No	No	No
No	No	No	No	No	No	No	No	No	No	No	No	No
No	No	No	No	No	No	No	No	No	No	No	No	No
No	No	No	No	No	No	No	No	No	No	No	No	No
No	No	No	No	No	No	No	No	No	No	No	No	No
Yes	No	No	No	Yes	Yes	No	No	No	No	No	No	No
No	No	Yes	Yes	No	No	No	No	No	No	No	No	No
No	No	No	No	No	No	No	No	No	No	No	No	No
No	No	No	No	No	No	No	No	No	No	No	No	No
No	No	No	No	No	No	No	No	No	No	No	No	No
No	No	No	No	No	No	No	No	No	No	No	No	No
No	No	No	No	No	No	No	No	No	No	No	No	No
No	No	No	No	No	No	No	No	No	No	No	No	No
No	No	No	No	No	No	No	No	No	No	No	No	No
Yes	Yes	No	No	No	No	No	No	No	No	No	No	No
No	No	No	No	No	No	No	No	No	No	Yes	Yes	Yes
No	No	No	No	Yes	Yes	No	No	No	No	Yes	Yes	No
No	No	No	No	No	No	Yes	Yes	No	Yes	No	No	No
No	No	Yes	Yes	No	No	No	No	No	No	No	No	No
No	No	No	No	No	No	No	No	No	No	No	No	No
No	No	No	No	No	No	No	No	No	No	No	No	No
2	1	2	2	2	2	2	2	1	2	2	2	2
N/A	No	N/A	Yes	N/A	No	N/A	No	N/A	No	N/A	No	N/A

N/A	No	N/A	No	N/A	No	N/A	No	N/A	No	N/A	No	N/A
N/A	No	N/A	No	N/A	No	N/A	No	N/A	Yes	N/A	No	N/A
N/A	No	N/A	No	N/A	No	N/A	No	N/A	No	N/A	Yes	N/A
N/A	Yes	N/A	No	N/A	Yes	N/A	Yes	N/A	No	N/A	Yes	N/A
N/A	Present	N/A	Partial	N/A	Present	N/A	Present	N/A	Partial	N/A	Partial	N/A

*ITSM

No	N/A	No	N/A	No	N/A	N/A	N/A	N/A	N/A	N/A	N/A	N/A
No	N/A	Yes	N/A	No	N/A	N/A	N/A	N/A	N/A	N/A	N/A	N/A
No	N/A	No	N/A	Yes	N/A	N/A	N/A	N/A	N/A	N/A	N/A	N/A
Yes	N/A	Yes	N/A	No	N/A	N/A	N/A	N/A	N/A	N/A	N/A	N/A
Present	N/A	Present	N/A	Partial	N/A	N/A	N/A	N/A	N/A	N/A	N/A	N/A

FESTER	FESTER	FESTER	FESTER	FESTER	FESTER	FESTER	FESTER	FESTER	FESTER	COREC	COREC	COREC
FF21	FF26	FF27	FF31	FF33	FF37	FF38	FF39	FF40	FF42	Co2A	Co2B	Co8
No	No	No	Yes	No	No	No	No	No	No	Yes	No	No
No	No	No	No	No	No	No	No	No	No	Yes	No	No
No	No	No	No	No	No	No	No	No	No	Yes	No	No
No	No	No	No	No	No	No	No	No	No	Yes	No	No
No	No	No	Yes	No	No	No	No	No	No	Yes	No	Yes
No	No	No	No	Yes	No	No	No	No	No	Yes	No	Yes
No	No	Yes	No	No	No	No	No	No	No	Yes	No	Yes
No	No	No	No	No	No	No	No	No	No	Yes	No	No
No	No	No	No	No	No	No	No	No	No	Yes	No	No
No	No	No	No	No	No	No	No	Yes	No	No	No	No
No	No	No	No	No	No	No	No	No	No	No	No	No
No	No	No	No	No	No	No	No	No	No	Yes	No	No
No	No	No	No	No	No	No	No	No	No	No	Yes	Yes
No	No	No	Yes	Yes	No	No	No	No	No	Yes	Yes	Yes
No	No	No	No	No	No	No	No	No	No	Yes	Yes	Yes
No	No	No	No	No	No	No	No	No	No	No	Yes	Yes
No	No	No	Yes	No	No	No	No	No	No	Yes	No	Yes
No	No	No	No	No	No	No	No	No	No	No	Yes	Yes
No	No	No	No	No	No	No	No	No	No	Yes	Yes	Yes
No	No	No	No	No	No	No	No	No	No	Yes	No	No
No	No	No	Yes	No	No	No	No	No	No	Yes	No	Yes
No	Yes	Yes	Yes	No	No	No	No	Yes	No	Yes	No	Yes
No	No	No	No	Yes	No	Yes	Yes	Yes	No	Yes	No	No
No	No	No	No	Yes	No	No	No	No	No	No	Yes	No
Yes	No	No	No	No	Yes	No	No	No	No	Yes	No	No
No	No	No	Yes	No	No	No	No	No	No	No	Yes	No
1	1	2	7	4	1	1	1	3	1	18	8	12
N/A	N/A	N/A	N/A	N/A	N/A	N/A	N/A	N/A	N/A	No	No	No

N/A	N/A	N/A	N/A	N/A	N/A	N/A	N/A	N/A	N/A	No	No	No
N/A	N/A	N/A	N/A	N/A	N/A	N/A	N/A	N/A	N/A	Yes	Yes	No
N/A	N/A	N/A	N/A	N/A	N/A	N/A	N/A	N/A	N/A	Yes	Yes	Yes
N/A	N/A	N/A	N/A	N/A	N/A	N/A	N/A	N/A	N/A	No	No	No
N/A	N/A	N/A	N/A	N/A	N/A	N/A	N/A	N/A	N/A	Present	Present	Present

ITSM

COREC	COREC	COREC	COREC	COREC	COREC	COREC	COREC	COREC	COREC	COREC	COREC	COREC
Co9	Co19	Co20	Co24	Co26	Co28	Co33	Co34	Co36	Co37	Co40	Co43	Co45
No	No	No	No	No	No	No	No	No	No	No	No	No
Yes	Yes	Yes	No	No	No	No	No	No	No	No	No	No
No	No	No	Yes	No	No	No	No	No	No	No	No	No
Yes	Yes	Yes	No	Yes	No	No	No	No	No	No	No	No
Yes	No	Yes	No	No	No	No	No	No	No	No	No	No
Yes	No	Yes	Yes	No	No	No	No	No	No	No	No	No
Yes	No	Yes	No	No	No	No	No	Yes	Yes	No	No	No
No	No	No	No	No	No	No	No	No	No	No	No	No
No	No	No	No	No	No	No	No	No	No	No	No	No
No	No	No	No	No	No	No	No	No	No	Yes	No	No
No	No	No	No	No	No	No	No	No	No	No	No	No
No	No	No	No	No	No	No	No	No	No	No	No	No
No	Yes	Yes	Yes	Yes	Yes	No	No	Yes	No	No	No	Yes
Yes	Yes	Yes	Yes	Yes	Yes	No	No	Yes	No	No	Yes	No
Yes	No	Yes	No	Yes	Yes	No	No	Yes	No	No	No	Yes
Yes	No	No	No	Yes	Yes	No	No	Yes	No	No	No	No
Yes	Yes	Yes	Yes	No	No	No	No	No	No	No	No	No
Yes	Yes	No	No	No	Yes	No	No	No	No	No	No	Yes
No	No	No	Yes	Yes	Yes	No	No	No	No	No	No	No
Yes	No	No	Yes	Yes	Yes	No	No	No	No	No	No	No
No	Yes	Yes	No	Yes	Yes	No	No	No	No	No	No	No
No	No	Yes	Yes	No	Yes	Yes	Yes	No	No	No	No	No
Yes	No	Yes	No	No	No	No	No	Yes	No	No	Yes	No
Yes	No	No	No	No	No	No	No	No	No	No	Yes	No
Yes	Yes	Yes	No	Yes	Yes	No	No	No	No	No	No	No
Yes	No	Yes	Yes	Yes	Yes	No	No	Yes	No	No	No	Yes
15	8	14	9	10	11	1	1	7	1	1	3	4
No	No	No	Yes	No	No	No	No	No	Yes	No	Yes	No

No	No	No	No	No	No	No	No	No	No	No	No	No
No	No	No	No	No	No	No	No	Yes	Yes	No	No	Yes
No	No	Yes	No	Yes	No	No	No	No	No	No	Yes	No
Yes	No	No	No	No	No	No	No	No	No	No	No	No
Present	Partial	Present	Partial	Partial	Partial	Partial	Partial	Present	Present	Partial	Partial	Present

COREC	COREC	COREC	COREC	COREC	COREC		
Co66	Co68	Co69	Co70	Co73	Co75	Total Festers	Total Fester-Coreceptors
No	No	No	No	No	No	9	9
No	No	No	No	No	No	11	11
No	No	No	No	No	No	10	10
No	No	No	No	No	No	10	12
No	No	No	No	No	No	10	13
No	No	No	No	No	No	11	13
No	No	No	No	No	No	9	12
No	No	No	No	No	No	9	7
No	No	No	No	No	No	10	8
No	No	No	No	No	No	11	6
No	No	No	No	No	No	7	4
No	No	No	No	No	No	10	10
No	No	No	No	No	No	10	28
No	No	No	No	No	No	10	19
No	No	No	No	No	No	11	26
No	No	No	No	No	No	7	18
No	No	No	No	No	No	10	15
No	No	Yes	No	No	No	13	17
No	No	Yes	Yes	No	Yes	7	20
No	Yes	Yes	Yes	Yes	No	7	15
No	No	No	No	No	No	19	20
No	No	No	No	No	No	22	20
No	No	No	No	No	No	18	16
Yes	No	No	No	No	No	12	12
No	No	No	No	No	No	17	16
No	No	No	No	No	No	12	17
1	1	3	2	1	1		
Yes	No	No	No	No	Yes		

No	No	No	No	No	No		
No	No	Yes	Yes	No	No		
No	No	No	Yes	Yes	Yes		
No	Yes	No	No	No	No		
Partial	Present	Partial	Partial	Partial	Partial		
						Fester genes	Fester-Coreceptor genes
						Average	10
						StD	2
							14
							6

Extended Data Table 4. Alternative splicing of *fester* genes

Fester genes	Number of alternative splice exons between Sushi and TM-I Domains	Number of alternative splice exons in the cytoplasmic region
FF1	2	Not detected
FF2	2	Not detected
FF3	2	Not detected
FF4	2	Not detected
FF5	1	Not detected
FF6	2	Not detected
FF7	3	Not detected
FF8	2	Not detected
FF9	2	Not detected
FF10	1-2	1
FF11	1	1
FF12/18/44	1	Not detected
FF13/15/16/19	1	Not detected
FF14	1	Not detected
FF17	1	Not detected
FF20	Not detected	Not detected
FF21	2	Not detected
FF22	2	2 (Introns)
FF23	2	1
FF24	2	1
FF25	Not detected	Not detected
FF26	2	1
FF27	Not detected	Not detected
FF28/29/30	2/1/Not detected	1
FF31	Not detected	Not detected
FF32	2	2
FF33	Not detected	Not detected
FF34	Not detected	1
FF35	2	1
FF36	Not detected	Not detected

FF37	2	1
FF38	Not detected	Not detected
FF39	Not detected	Not detected
FF40	Not detected	Not detected
FF41	2	Not detected
FF42	Not detected	Not detected
FF43	Not detected	Not detected
FF45	1	1